An-Najah National University

Faculty of Graduate Studies

ENERGY CONSUMPTION EVALUATION OF ABSORPTION-COMPRESSION HYBRID REFRIGERATION SYSTEM FOR COLD STORAGE

By

Ibrahim Abdelrahim Mohammad Amayreh

Supervisor

Dr. Abdelrahim Abusafa

This Thesis is Submitted in Partial Fulfillment of the Requirements for the Degree of Master of Clean Energy Conservation Engineering, Faculty of Graduate Studies, An-Najah National University, Nablus-Palestine.

2024

ENERGY CONSUMPTION EVALUATION OF ABSORPTION-COMPRESSION HYBRID REFRIGERATION SYSTEM FOR COLD STORAGE

By

Ibrahim Abdelrahim Mohammad Amayreh

This Thesis was Defended Successfully on 20/08/2024 and approved by:

Dr. Abdelrahim Abusafa	
Supervisor	Signature
Dr. Ishaq Sider	
External Examiner	Signature
Dr. Mohammed Alsayed	
Internal Examiner	Signature

Dedication

In profound gratitude to Allah, the source of strength and guidance, I dedicate this work to my beloved country, Palestine.

To the resilient people of Palestine, who endure with unwavering courage and determination in the face of adversity. Your enduring spirit and commitment to justice inspire me, and it is with great honor that I dedicate this thesis to the land that has shaped my identity and values.

To my parents, family, friends, students, and colleagues, your support has been my anchor. This dedication extends to you, as well, for being a part of this journey and contributing to its significance.

May this work serve as a testament to the enduring spirit of Palestine and its people, reflecting the resilience, strength, and unwavering hope that define our homeland.

Acknowledgements

I extend my deepest gratitude to the following individuals and institutions whose support and contributions have been instrumental in the completion of this thesis:

To my beloved parents and my cherished family, whose unwavering love, encouragement, and sacrifices have shaped the person I am today. Your support has been the cornerstone of my accomplishments, and I dedicate this work to you with heartfelt gratitude.

I'm profoundly thankful to my teachers, specifically my supervisor, Dr. Abdelrahim Abusafa, for his guidance, expertise, and unwavering support throughout the entire research process. his insightful feedback and encouragement have been invaluable.

I extend my gratitude to my friends and colleagues who provided valuable insights, engaging discussions, and a supportive academic community. Your camaraderie made the research journey more enjoyable.

To my dedicated students, who have been a source of inspiration and a reminder of the profound impact education can have on lives. Your curiosity and enthusiasm fuel my passion for teaching.

I would like to acknowledge the An-Najah National University for providing resources, facilities, and a conducive environment for academic exploration.

Special thanks to Palestine Polytechnic University for their support and encouragement in providing the necessary facilities to complete my educational journey.

May this work stand as a token of my appreciation and gratitude to all those who have played a part, big or small, in this academic pursuit.

Declaration

I, the undersigned, declare that I submitted the thesis entitled:

ENERGY CONSUMPTION EVALUATION OF ABSORPTION-COMPRESSION HYBRID REFRIGERATION SYSTEM FOR COLD STORAGE

I declare that the work provided in this thesis, unless otherwise referenced, is the researcher's own work, and has not been submitted elsewhere for any other degree or qualification.

Student's Name: Ibrahim Amayreh

Signature: 

Date: 20/08/2024

List of Contents

List of Tables

List of Figures

List of Appendices

ENERGY CONSUMPTION EVALUATION OF ABSORPTION-COMPRESSION HYBRID REFRIGERATION SYSTEM FOR COLD STORAGE

By

Ibrahim Abdelrahim Mohammad Amayreh

Supervisor

Dr. Abdelrahim Abusafa

Abstract

Numerous interrelated variables that affect the environment, the economy, and the welfare of the world at large need the use of renewable energy. Accordingly, the Absorption Compression Hybrid Refrigeration System (ACHRS) is studied in this research. Given the high cost of electrical energy and the climate that is conducive to solar energy collection, it seemed more practical and economically feasible to find a different way to operate cold storage while maintaining system performance. ACHRS merges the Vapor Compression Refrigeration System (VCRS), and Absorption Refrigeration System (ARS), Based on the temperature of the water after it has been heated with evacuated tube solar water collectors, if the water temperature is 90 ℃ and more, the system will operate by ARS, else by VCRS. The study's results demonstrated the annual working hours for the hybrid system will be 2078 by ARS and 6682 by VCRS. The hybrid system payback period is 5.6 years. Net Cash Flow (NCF), and Internal Rate of Return (IRR) are other methods to assess the economic viability that have been studied, through these, the system's economic viability was demonstrated.

Keywords: Absorption Refrigeration; Economic Feasibility; Evacuated Tube Collectors; Hybrid Refrigeration; Solar Energy.

Chapter One

Introduction and Theoretical Background

1.1 Introduction and Overview

Refrigeration is essential to increase the perishable goods' shelf life such as fruits, vegetables, dairy, meat, and seafood. Its use is widespread across a number of sectors, including logistics, food processing, pharmaceuticals, and agriculture. In cold storage, cooling serves the main purpose of preserving low temperatures that prevent the growth of germs and delay the enzymatic and chemical reactions that cause spoiling.

Agricultural crops quickly begin to deteriorate after being harvested because they are cut off from their source of nourishment and water. They lose their appeal, nutritive value, texture, flavor, and weight. The deterioration of post-harvest products is influenced by temperature and time. Experts estimate that because producing farms and consumption centers lack preservation facilities, over one-third of all perishable goods never reach the consumer globally (Jog, 2004). By reducing the rate of respiration, cooling the harvested products in a cold store helps to control the rate of quality loss (Agyenim, 2007).

Perishable agricultural products can be stored in the cold storage, a structure featuring thermal insulation and a refrigeration system, for varying periods of time while maintaining the proper humidity and temperature levels. The rate of deterioration and spoiling that would naturally occur in an uncontrolled natural environment is reduced by such storage under controlled conditions (Abd et al., 2017).

The increasing demand for ecologically friendly refrigeration systems has led many researchers to focus on absorption cooling research in recent years. The severity of chlorofluorocarbons (CFCs) and (hydrochlorofluorocarbons) HCFC induced ozone depletion has led to a rapid advancement in CFCs free refrigeration and air conditioning technology. Restructuring energy use practices to improve efficiency is necessary to prevent global warming, and to minimize the global warming potential (GWP). From this vantage point, the fact that absorption refrigeration can reduce the amount of electricity produced from fossil fuels and does not require the use of ozone depleting refrigerants has drawn the interest of numerous researchers in the field.

Heat is the energy input for vapor absorption cooling systems as opposed to mechanical work for the vapor compression refrigeration systems. In large power plants and factories, heat is a low-grade energy source that is easily accessible as waste. Other energy sources that provide it include geothermal, biomass, solar, and others (Fadiel & Esham, 2023).

1.2 Literature Review

The absorption refrigeration system has attracted a lot of interest because it has the potential to provide refrigeration solutions that are both environmentally friendly and energy-efficient, especially when combined with other energy systems. To increase performance and adaptability under a variety of operating situations, a hybrid absorption refrigeration system usually combines absorption cycles with other systems, such as vapor compression, solar thermal energy, biomass, or waste heat recovery units.

Although this topic hasn't been studied before, there have been many other studies on absorption-compression hybrid refrigeration systems from different perspectives, some of which are related to the type of renewable energy, others to the utilization of the condenser heat that is rejected to the ambient in the compression refrigeration system, and others to the working fluid. Traditional absorption refrigeration systems require the generator to be supplied with high-temperature heat, while a significant amount of low-temperature heat is immediately rejected to the environment through the condenser and the absorber.

Wang et al. (2016) research sought to improve the efficiency of traditional air-conditioning systems by recovering all condensation heat used in the production of refrigerant and enhancing its quality using a vapor compressor. The generating heat input from the outside is reduced by 70–80% when condensation heat is recovered for generation by an absorption–compression hybrid refrigeration system. The new system's primary energy efficiency is also up to 97.1% greater than that of conventional absorption refrigeration system.

Gado et al. (2021) examines three configurations of a solar-driven hybrid adsorption-compression cooling system for their energy and financial viability. In configuration No.1 (as shown in Figure A.1 in Appendix A), the vapor compression system is electrically powered, while the adsorption system is powered by solar collectors. The

vapor compression cycle in configuration No.2 (as shown in Figure A.2 in Appendix A) is powered by additional photovoltaic panels, creating a net-zero electricity consumption system. Between the adsorption and compression subsystems, configuration No.3 (as shown in Figure A.3 in Appendix A) is equipped with an additional cold storage tank for extended operation. The MATLAB/Simulink platform is used to create mathematical models, which are then tested against experimental data from the most pertinent literature. Theoretical findings for configuration No.1 show that by increasing the size ratio between the adsorption and compression systems from 0.867 to 1.333, the electricity usage in June decreases from 22.37 kWh to 5.9 kWh. When compared to the traditional vapor compression system, configuration No.1 can significantly reduce the electricity consumption by 62.5%. Additionally, it has been discovered that configuration No.2 can reduce electrical energy use by up to 2897 kWh per year. configuration No.3 achieves yearly energy savings of 47% as opposed to configuration No.1 64%, although it operates for longer periods of time, which is a positive. Additionally, economic analyses are done for the three configurations under consideration, and configuration No.2 economic viability is demonstrated by its 9.65-year payback period. These findings might encourage designers and other interested parties to choose novel hybrid cooling systems over the more common compression cooling techniques.

Han et al. (2013) suggests a novel mid-temperature waste heat-powered hybrid absorption-compression refrigerator. The system's working fluid is a binary mixture of ammonia and water. It comprises of two refrigeration subsystems: absorption refrigeration and heat-driven compression refrigeration. The cascade utilization of waste heat in the two subsystems in the new system results in higher performance. When compared to a traditional ammonia-water absorption refrigerator, the suggested system produces 46.7% more cooling energy from the same amount of waste heat input. The technology can be used to produce cooling using waste heat in an effective manner.

A cryogenic refrigeration system and a vapor compression refrigeration system make up the hybrid cooling system. In this study, the researchers Gazda & Kozioł (2013) examines the hybrid refrigeration system's energy efficiency. Results show that the air blast-cryogenic freezing method's coefficient of performance is higher than that of air

blast freezing with a compression refrigeration system and lower than that of cryogenic freezing with a cryogenic refrigeration system.

A thorough analysis of absorption refrigeration technologies was provided by Srikhirin et al. (2001), who also provided insightful information on the classifications, refrigerant-absorbent pairs, system configurations, and operating principles of both well-known and up-and-coming absorption systems. The research stressed the appropriateness of absorption systems in settings where low-grade heat sources, such as solar thermal, waste heat, or biomass, are readily available. The authors methodically addressed both single-effect and double-effect absorption cycles, and compared the performance, efficiency, and application ranges of commonly used working pairs such as LiBr/H_2O and NH_3/H_2O. Their analysis identified LiBr/H_2O as particularly effective for air conditioning and cooling applications in climates with consistent solar radiation, while NH_3/H_2O was recognized for its ability to operate at lower temperatures, making it ideal for refrigeration and freezing applications. Technical issues that can impact the long-term operation of absorption chillers, including crystallization, corrosion, and system stability, were also discussed in the review. Srikhirin underlined that, although absorption systems have lower COPs than typical vapor compression systems, their environmental advantages—including zero ozone depletion potential and lower greenhouse gas emissions—make them a tempting option for sustainable cooling solutions. Furthermore, the authors called attention to the economic and engineering trade-offs involved in adopting these systems, noting the importance of system integration, component optimization, and control strategies to improve their feasibility for widespread adoption.

Liu et al. (2019) discuss the performance of two absorption compression hybrid refrigeration systems by comparing different working pairs. It was suggested to use the three new working pairs R1234yf/[HMIM] [TfO], R1234yf/[HMIM][PF6], and R1234yf/[HMIM][BF4]. The results demonstrate that the two systems can significantly enhance the cooling performance of the single effect absorption refrigeration system, including raising the coefficient of performance, lowering the condenser and circulation ratio's heat load, and expanding the range of operation for the generation temperature, absorption temperature, and evaporation temperature. The compressor should be placed between the evaporator and the absorber rather than the generator and the condenser.

Compared to R1234yf/[HMIM][PF6] and R1234yf/[HMIM][BF4], R1234yf/[HMIM][TfO] exhibits greater cooling performance.

Energy demand is rising as a result of new technology, and it doesn't seem to be slowing down anytime soon. A lot of environmental issues are being caused by excessive energy use, which is endangering energy depletion. Therefore, Selvaraj & Victor (2021) are examines and contrasts a renewable integration technology with a commercial AC absorption refrigeration system in which a solar photovoltaic system is employed to provide the electrical energy necessary to operate an absorption cycle. The AC and DC systems' respective Coefficients of Performance (COP) were 0.18 and 0.14. The system has a straightforward payback period of 10.2 years.

Hackett et al. (2005) in their research, that significant energy-saving opportunities exist in both large and small facilities, especially in their refrigeration systems. Despite the limited number of samples for both smaller and bigger size plants, it was discovered that the smaller plants benefited in both categories of high-efficiency refrigeration equipment and refrigeration system control and optimization. However, the control and optimization of refrigeration systems greatly benefits larger facilities. Additional areas where cost savings are feasible include lighting, boiler systems, motor drives and control, and time-of-use refrigeration load-shifting.

He & Chen (2007) studied auto-cascade absorption refrigeration (ACAR) and contrasted it with conventional absorption systems, demonstrating that under identical operating conditions, the ACAR system may achieve a significantly lower refrigerating temperature. With the use of low-potential thermal power, the novel ACAR system achieves one of the lowest refrigerating temperatures ever attained by an absorption refrigeration system. This temperature is ideal for deep freezing at temperatures as low as 50 °C. The obtained COP is not high considering that this experimental system is the first prototype of the ACAR cycle.

Basu & Ganguly (2016) studied a design of a cold storage for potatoes, the system runs on electrical energy produced by solar thermal and photovoltaic sources. It is discovered that the payback periods for both the thermal and photovoltaic components are under four years. The combined thermal and photovoltaic integrated power system has a net yearly energy surplus of roughly 36.062 MWh.

Bux & Ansari (2017) research demonstrated that the vapor absorption refrigeration cycle, when employed in the summer, can effectively produce a refrigeration effect using a solar flat plate collector water heater. Furthermore, the temperature of the hot water supplied to the generator determines how much of a refrigeration effect there will be.

Globally, the building sector's energy consumption has significantly increased due to the growing need for air conditioning, especially during the summer. In Europe, where air conditioning installations have rapidly expanded in both residential and commercial buildings, this tendency is particularly noticeable by Balaras et al. (2007) in their studies. Solar-assisted air conditioning has become a viable substitute in response to this increasing demand and the resulting stress on electricity infrastructure. By combining solar thermal collectors with heat-driven cooling technologies, these systems provide the twin advantages of lowering electricity use and lessening environmental effects.

The different technological routes for transforming solar energy into refrigeration, including solar electric, solar thermal, and hybrid systems, were thoroughly categorized and assessed by Kim & Infante Ferreira (2008) in their thorough review. Solar photovoltaic (PV) systems, which use electricity from solar panels to power traditional vapor compression refrigeration cycles, and solar thermal systems, which use thermodynamic cycles to transform thermal energy into cooling, are the two primary categories into which solar-driven refrigeration technologies are typically divided. The latter comprises desiccant, absorption, adsorption, and thermo-mechanical cooling systems; each has unique operational features and appropriateness based on application, scale, and climate. Solar electric and thermo-mechanical systems are comparatively easy to incorporate into traditional infrastructure and provide significant operating flexibility. However, because these systems require electrical components like compressors, batteries, and inverters, they have greater capital expenses. However, when combined with thermal collectors, solar thermal sorption systems specifically, absorption and adsorption systems have proven to be more economically viable, particularly in medium to large scale applications. In terms of cost and performance, absorption refrigeration systems have shown the most promise, especially those that use lithium bromide water ($LiBr–H_2O$) as the working fluid. These systems have

comparatively high Coefficients of Performance (COP) for single-effect units, usually between 0.6 and 0.8, and can function well with low-temperature heat sources, such as evacuated tube solar collectors or flat plate solar collectors. Furthermore, these systems are thought to have the lowest overall cost of all the technologies examined, which makes them suitable for use in home and institutional cooling applications. According to the researcher's comparative analysis, single-effect absorption systems provide the best balance between cost, energy efficiency, and system simplicity among the many solar cooling solutions.

The development of a 5kW ammonia-water absorption chiller for solar cooling applications is presented in Boudéhenn et al. (2012). the selection of the most affordable, small-diameter, low-ammonia heat-loading flat plate heat exchangers on the market is based on these factors. Even in the case of a prototype, the various technical options allow for the construction of a compact chiller with low solution and refrigerant quantities. The initial experimental findings are highly promising. However, additional areas for optimization have been found, particularly with regard to the absorber and the solution heat exchanger. Recent experimental tests using modified control strategies yielded results that were nearly in line with numerical expectations.

1.3 Meteorological Data

The National Solar Radiation Database (NSRDB) provides free time series weather data for many countries of the world. It is managed by the National Renewable Energy Laboratory (NREL), which is a part of the United States department of energy. With a growing list of international locations and high temporal (15 min) and spatial (4 km) resolutions to accurately represent global and regional solar radiation climates, the NSRDB is one of the most accessed public datasets offering a serially complete collection of solar energy and meteorological data, including the three most common measurements of solar radiation: global horizontal, direct normal, and diffuse horizontal irradiance (Sengupta et al., 2018).

Jericho is the site of the research. Jericho is a Palestinians situated at latitude 31.85°N and longitude 35.46°E, located -227 meters below sea level, east of the West Bank. According to NSRDB It is situated in an area with a hot desert climate and high mean temperature. In this city, summertime temperatures can reach 40°C, which is extremely

hot. The average temperature in 2019 was estimated to be 24.5°C, and the average global horizontal solar radiation is 5.43 kWh/m^2/day.

People in this city complain about the high energy consumption required to operate cold rooms in general, as the temperature difference between the inside of the cold rooms and their surroundings is significantly high, which increases the rate of heat transfer unless there is ideal insulation. The high energy consumption is due to the operation of systems that operate using vapor compression refrigeration systems by the compressor work and defrost electrical heaters.

The meteorological data for Jericho was obtained from NSRDB website at link (https://nsrdb.nrel.gov/data-viewer) for the year 2019, the data files include measurement data at 30-minute intervals. It contains the global horizontal solar radiation and the ambient air-dry bulb temperature, as well as all other solar and meteorological data. This file export to System Advisor Model (SAM) software.

The National Renewable Energy Laboratory (NREL) in the United States created the System Advisor Model (SAM), a program for financial and performance modeling. Its purpose is to assist in the planning, analysis, and assessment of renewable energy systems. Solar photovoltaic (PV), solar thermal (CSP), wind, geothermal, and biomass systems are just a few of the renewable energy technologies that SAM users can model. Its capacity to combine thorough financial analysis tools with in-depth system performance modeling is one of its main advantages, allowing users to evaluate the technical and financial viability of renewable energy projects.

Along with financial considerations like capital cost, operation and maintenance (O&M) costs, and electricity tariffs, SAM enables users to enter site-specific information like solar irradiance, temperature, and wind speed. The model is very relevant for both utility-scale and distributed energy applications since it offers a variety of finance mechanisms (such as loans, power purchase agreements, and third-party ownership).

SAM is frequently used in engineering design, project development, and academic research because of its clear structure, frequent updates, and robust documentation. SAM was used in this study to assess the financial benefits and energy efficiency of hybrid renewable systems for cold storage applications. It was a crucial tool for scenario

comparison and decision-making because of its capacity to incorporate financial measures like payback period (SPP), internal rate of return (IRR), and net present value (NPV) and simulate hourly performance.

Figure 1.1 shows the exported annual distribution of the ambient temperatures and global irradiance in Jericho, and Figure 1.2 shows the exported distribution of the Jericho ambient temperatures and global irradiance per month.

Figure 1.1

Annual distribution of the ambient temperatures and global irradiance in Jericho

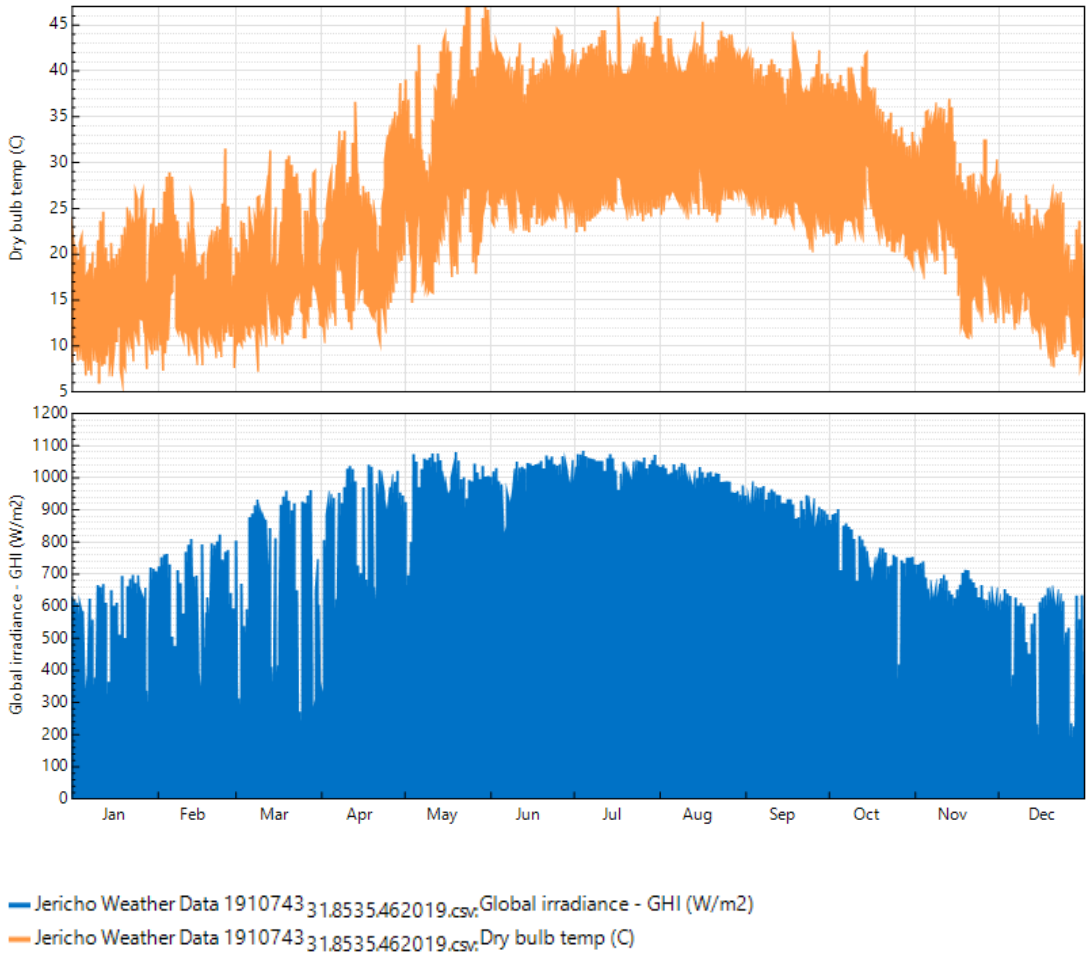

The annual variation in Jericho's global horizontal irradiance (GHI) and ambient dry-bulb temperature is shown in Figure 1.1. While the lower graph displays the comparable hourly global irradiance (W/m^2), the upper graph depicts the hourly variations in dry-bulb temperature (°C) over the course of the year. With values ranging from roughly 10°C in the winter (January and December) to a maximum above 45°C in the summer (June to August), the temperature profile clearly shows a seasonal trend. The

performance of thermal energy-driven systems, such as the Absorption Refrigeration System (ARS), is significantly impacted by this large range, which emphasizes the considerable thermal load variation anticipated throughout the year. Similar seasonal trends can be seen in the GHI data, where daily irradiance levels rise from about 500 W/m^2 in January to over 1000 W/m^2 in mid-summer (April to August). The viability of using solar thermal energy in late spring and summer is supported by the constant high irradiance levels during these seasons. Nevertheless, the significant decrease in GHI during the winter months restricts the amount of solar energy available for solar-dependent systems to run continuously. Overall, Jericho has a hot, dry environment with significant solar potential, especially between April and October.

The monthly diurnal profiles of global horizontal irradiance (GHI) and ambient dry-bulb temperature (°C) in Jericho are shown in Figure 1.2, where each subplot corresponds to a distinct month of the year. The orange curves track the ambient temperature (°C) over a 24-hour period, whereas the blue curves show GHI in (W/m^2). All month long, the GHI curves display a clear bell-shaped profile that peaks at midday, or the sun's highest point in the sky, usually between 12:00 and 14:00. The summer months (April to August) have maximum GHI values over 1000 W/m^2, with May and June exhibiting the highest levels of sun irradiance. On the other hand, the GHI maximum are much lower during the winter months of December and January, typically falling between 500 and 700 W/m^2, which suggests less solar availability. A typical daily heat cycle is also seen in the ambient temperature curves, which peak in the afternoon after increasing gradually after sunrise. Peak temperatures during the summer months of May through September are close to or higher than 40°C, with July and August being the hottest. The winter months, on the other hand, saw substantially lower maxima, with highs of 15°C to 20°C and lows of 10°C or somewhat lower at night. Both solar irradiance and ambient temperature exhibit a seasonal and diurnal pattern, with their peaks closely aligned during the day, as demonstrated by the annual profile in the lower-left quadrant, which aggregates the trends over all months. When evaluating the feasibility of solar-powered systems, these profiles are essential. According to the data, solar thermal energy is plentiful in the summer, which makes it the perfect time of year to run an Absorption Refrigeration System (ARS). To guarantee consistent cooling performance throughout the year, a backup or hybrid system is necessary due to the wintertime decline in solar intensity and ambient temperatures.

Figure 1.2

Monthly distribution of the ambient temperatures and global irradiance in Jericho

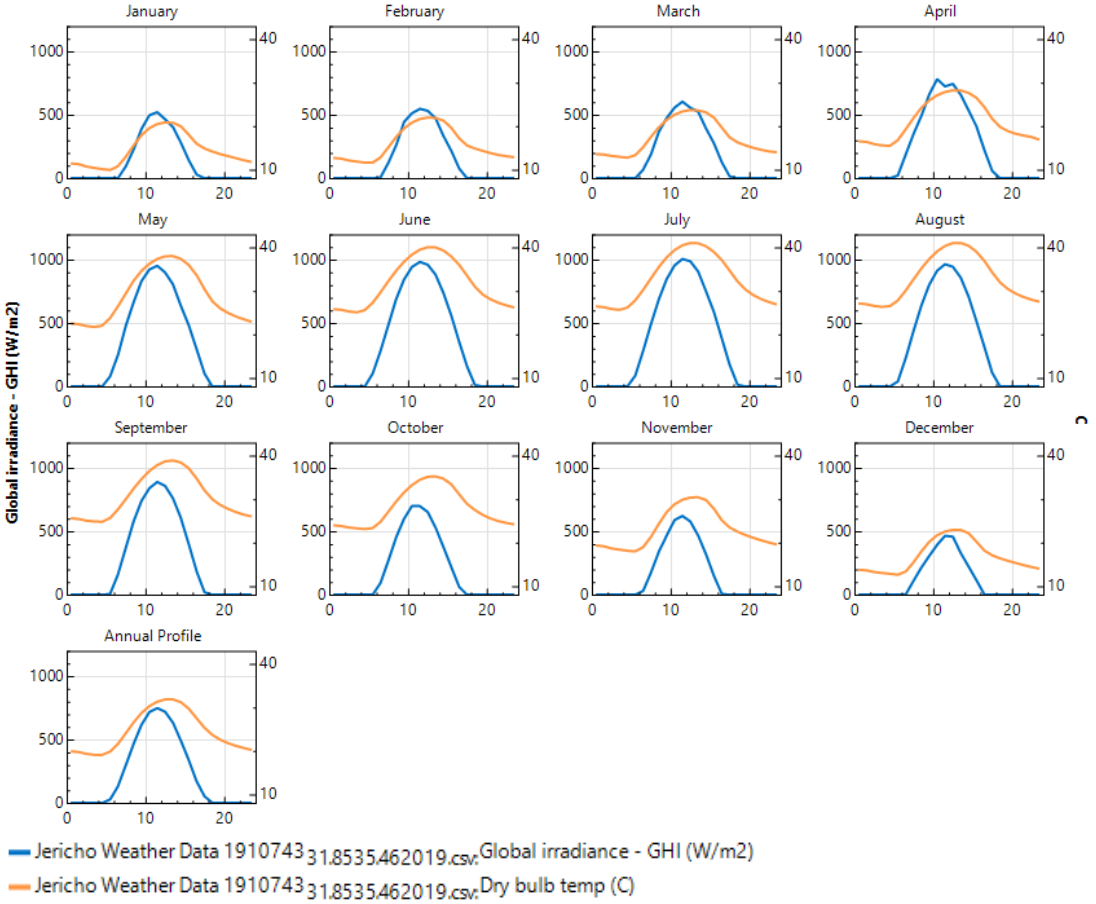

1.4 Ammonia Refrigerant

One of the oldest and most popular natural refrigerants in the world, ammonia (NH_3) is prized for its superior thermodynamic qualities, energy efficiency, and environmental friendliness. Chemically referred to as anhydrous ammonia, it finds widespread application in industrial refrigeration systems as well as in more environmentally friendly cooling technologies, such as absorption refrigeration cycles.

Ammonia, commonly referred to by the designation R717 as per the refrigerant naming conventions outlined by the American Society of Heating, Refrigerating and Air-Conditioning Engineers (ASHRAE), has a strong odor and is a colorless, low-density gas at room temperature. With a molecular mass of 17.03 g/mol, it is less dense than atmospheric air. At 25°C, it may be transported and kept as a liquid at a pressure of 1 MPa. Ammonia has a critical point of 11.3 MPa and 132.3°C. The mass per unit volume is 235 kg/m3 Herold et al. (2016). Ammonia has a boiling point of -33.32°C at

atmospheric pressure. It is deemed to have a lower flammability limit, and the auto-ignition temperature is 630°C.

Ammonia's high latent heat of vaporization, which enables it to absorb large amounts of heat during phase shift and produce extremely effective heat transfer, is one of its main advantages as a refrigerant. Furthermore, compared to many synthetic refrigerants, ammonia systems can attain greater coefficients of performance (COP) and run at comparatively lower mass flow rates. Because of these qualities, ammonia can be used in large-scale cooling applications such district cooling systems, ice plants, food processing facilities, and cold storage warehouses.

Ammonia is considered environmentally friendly because both of the Ozone Depletion Potential (ODP) and the Global Warming Potential (GWP) are zero. This makes it an attractive choice for companies and industries aiming to reduce their environmental impact. Despite being a useful refrigerant, ammonia is poisonous and should be handled carefully. Working with ammonia refrigeration systems necessitates the use of appropriate safety precautions, such as adequate ventilation and leak detection systems. Exposure to ammonia at high doses might be fatal. According to IPCS 1990, ammonia is flammable and explosive when it makes up 16–25% of the air's volume. Understanding each of these concerns is essential for safe use.

Big industrial refrigeration systems, in low and medium-temperature refrigeration such as those in ice rinks, cold storage warehouses, and food processing facilities, frequently employ ammonia. Furthermore, heat pumps and air conditioners use it.

Ammonia is an excellent copper solvent. It is therefore problematic to use any material that contains copper. Experiments conducted in the lab have shown that ammonia corrosion can occur in brass parts even plated with chromium. Stainless steel or carbon steel are the most often used materials in the construction of ammonia/water systems. For the majority of applications, corrosion inhibitors are necessary when using carbon steel. These salts are added in trace amounts (less than 1% of the total weight). On the metal surface, they create a shielding oxide layer to prevent direct contact with the working fluid. Usually, little consideration is given to how these salts affect the working fluid's thermodynamic characteristics. Steel has a thermal conductivity that is roughly ten times lower than copper's. Therefore, in comparison to copper, the wall material's

heat transfer resistance has a greater influence on heat exchanger design (Herold et al., 2016).

Ammonia-water and water-lithium bromide have been the most often utilized refrigerant-absorbent combinations appropriate for absorption systems. The water-lithium bromide absorption cycles are frequently used for air conditioning due to their advantageous working conditions, whereas the ammonia-water absorption cycles are primarily utilized for refrigeration temperatures below 0 °C (Hera et al., 2010) . Ammonia functions as the refrigerant and water as the absorbent in these systems. This combination works particularly well for low-temperature uses, such as off-grid solar cooling and ice production. Because NH_3-H_2O absorption systems can be driven by biomass, waste heat, or solar thermal energy, they can be installed in rural or isolated locations without consistent access to electricity.

1.5 Vapor Compression Refrigeration System

The vapor compression refrigeration system (VCRS), which finds use in commercial, industrial, and domestic refrigeration applications, is the most widely utilized refrigeration technology globally. Its basic idea is to use mechanical work, usually provided by an electrically powered compressor, to extract heat from a low-temperature area and reject it to a higher-temperature environment. The evaporator, expansion valve (or throttling device), compressor, and condenser are the fundamental parts of a VCRS, and they all function in a closed loop.

By fully vaporizing the refrigerant before it is compressed and substituting a throttling device, like an expansion valve or capillary tube, for the turbine, many of the impracticalities related to the reversed Carnot cycle can be avoided. This cycle, which is schematically illustrated in Figure 1.3, is known as the ideal vapor-compression refrigeration cycle. The most common cycle for heat pumps, air conditioners, and refrigerators is the vapor-compression refrigeration cycle. There are four processes involved:

1. 1-2 Isentropic compression in a compressor
2. 2-3 Constant-pressure heat rejection in a condenser
3. 3-4 Throttling in an expansion device

4. 4-1 Constant-pressure heat absorption in an evaporator

Figure 1.3

The ideal vapor compression refrigeration cycle schematic

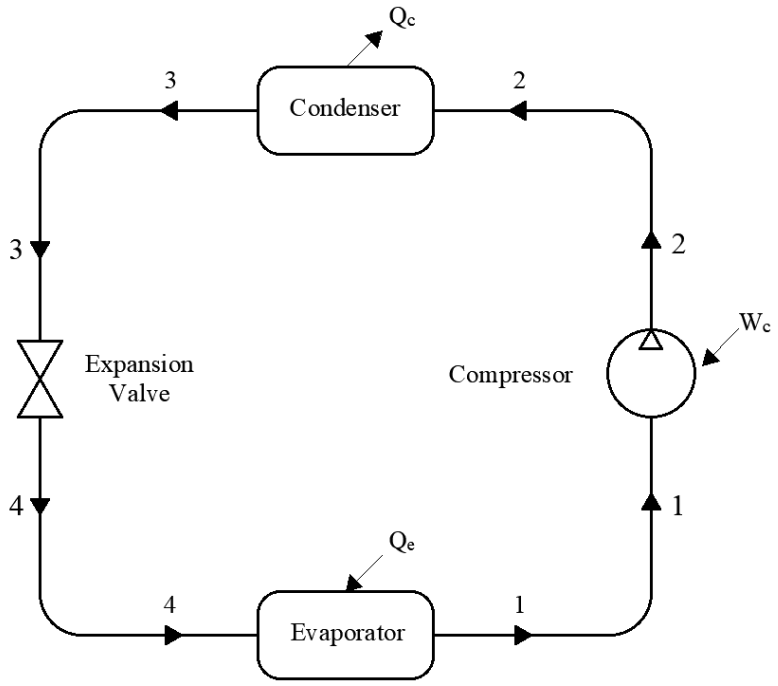

The refrigerant enters the compressor at state 1 as saturated vapor in an ideal vapor-compression refrigeration cycle, and it is compressed isentropically to the condenser pressure. During this isentropic compression process, the temperature of the refrigerant rises to a level significantly higher than that of the surrounding medium. After that, at state 2, the refrigerant enters the condenser as superheated vapor, and at state 3, heat rejection to the environment causes it to exit as a saturated liquid. At this point, the refrigerant's temperature is still higher than the ambient temperature. Using a capillary tube or expansion valve, the saturated liquid refrigerant in state 3 is throttled to the evaporator pressure. During this process, the temperature of the refrigerant falls below the temperature of the refrigerated space. At state 4, the low-quality saturated mixture of refrigerant enters the evaporator and evaporates entirely by absorbing heat from the refrigerated space. After exiting the evaporator as saturated vapor, the refrigerant enters the compressor once more to complete the cycle (Çengel & Boles, 2014).

Because of their great efficiency, dependability, and small size, VCR systems are preferred. Applications for them are numerous and include everything from air conditioners and refrigerators in homes to chillers, industrial cold storage units, and

refrigeration in vehicles. Their energy usage, however, is an issue, especially in hotter regions where the cooling burden is greatly increased by high ambient temperatures. The compressor must exert more effort to maintain the temperature differential between the cold room's interior and the surrounding air in locations like Jericho, where temperatures can rise beyond 40°C. Higher operating expenses and higher electricity consumption result from this.

Furthermore, synthetic refrigerants like CFCs, HCFCs, or HFCs which contribute to ozone depletion and global warming are frequently used in conventional VCR systems. The industry is increasingly shifting toward eco-friendly alternatives, such as natural refrigerants like ammonia (NH_3), carbon dioxide (CO_2), and hydrocarbons, as a result of environmental legislation and international accords like the Montreal Protocol and the Kigali Protocol. Even with these improvements, there are still sustainability issues with the VCR system, especially in places that are off the grid or have limited energy. In order to lessen grid reliance and their negative effects on the environment, there is increasing interest in combining VCR systems with renewable energy sources (like as photovoltaics) or hybridizing them with absorption refrigeration systems. However, in many rural or underdeveloped areas where power availability is expensive or sporadic, VCR systems are less appropriate due to their intrinsic need on electricity and mechanical parts like compressors and fans.

1.6 Absorption Refrigeration System

An eco-friendly and energy-efficient substitute for the traditional vapor compression refrigeration system (VCRS) is the absorption refrigeration system (ARS), a thermally powered cooling technology. The ARS uses thermal energy, which is frequently obtained from waste heat, solar thermal collectors, geothermal energy, or biomass combustion, to support the refrigeration cycle, in contrast to the VCRS, which depends on mechanical energy (electricity) to operate a compressor. Absorption refrigeration is especially attractive for off-grid, low-energy, or renewable energy-based applications because of this feature. An absorption refrigeration system is considered a “heat-driven” system. It has the unusual ability to convert thermal energy into refrigeration power directly. A solution comprising a refrigerant and an absorbent with a strong chemical affinity for one another serves as the system's working fluid. Absorption refrigeration is a different type of refrigeration that becomes economically viable when a source of

cheap thermal energy at a temperature of 100 to 200°C is available. Geothermal energy, solar energy, waste heat from cogeneration or process steam plants, and even relatively cheap natural gas are a few examples of low-cost thermal energy sources. Absorption refrigeration systems, as the name suggests, entail the absorption of a refrigerant by a transport medium. The ammonia–water system, which uses water (H_2O) as the transport medium and ammonia (NH_3) as the refrigerant, is the most popular absorption refrigeration system. Water-lithium chloride and water-lithium bromide systems are examples of additional absorption refrigeration systems in which water is the refrigerant. The latter two systems can only be used in situations where the minimum temperature is higher than the freezing point of water, such as air conditioning.

Five major parts make up the absorption system: the absorber, evaporator, expansion valve, condenser, and generator. Instead of using a mechanical compressor, ARS uses a thermal compressor, which is basically a generator and absorber combined. Heat is delivered to a solution consisting of a refrigerant and an absorbent (often ammonia-water (NH_3-H_2O) or lithium bromide-water (LiBr-H_2O) in the generator to start the cycle. The refrigerant separates from the absorbent due to vaporization caused by the heat input. After that, the high-pressure refrigerant vapor enters the condenser, where it condenses into a liquid and rejects heat to the environment. The low-pressure refrigerant enters the evaporator after going through the expansion valve. There, it absorbs heat from the cooled area and evaporates to create the necessary refrigeration effect. The absorbent solution then reabsorbs the vapor after it has entered the absorber. After the cycle is finished by this exothermic process, the solution is pumped back to the generator so that the cycle can continue.

In order to comprehend the fundamental concepts of absorption refrigeration, an illustration of the NH_3-H_2O system can be found in Figure 1.4. The system is similar to the vapor-compression system, as can be seen in the figure, but instead of a compressor, there is a sophisticated absorption mechanism that consists of an absorber, a pump, a generator, a regenerator or heat exchanger, a valve, and a rectifier. The components in the box are only meant to raise the pressure of NH_3, heat from the refrigerated space is absorbed as it passes through the evaporator, where it is cooled and condensed in the condenser by rejecting heat to the surroundings.

Figure 1.4

NH_3-H_2O absorption refrigeration cycle schematic

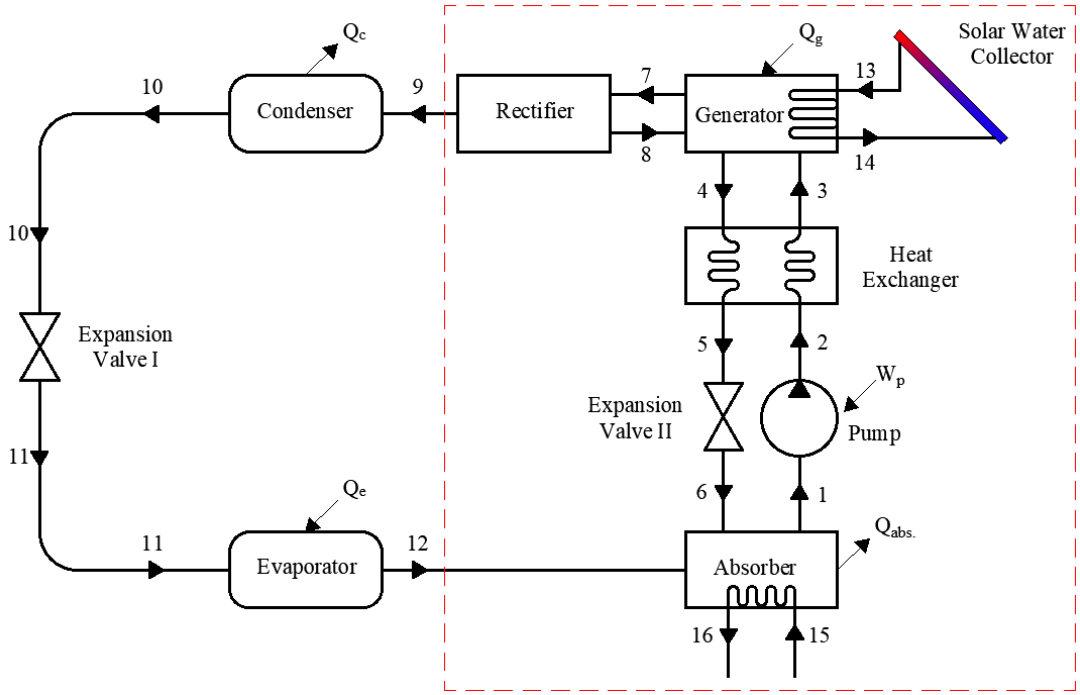

Thus, nothing new has been added. This is what transpires inside the box: After exiting the evaporator, ammonia vapor goes into the absorber where it dissolves and combines with water to create NH_3-H_2O strong solution, rich with NH_3. Since this reaction is exothermic, heat is released throughout. Temperature and the amount of NH_3 that can dissolve in H_2O are inversely correlated. In order to maximize the amount of NH_3 dissolved in water, it is necessary to cool the absorber and keep its temperature as low as possible. The strong solution pumped to the regenerator which transfers some heat to the rich solution exiting the pump, and weak solution, poor with NH_3, which exiting of the generator. The generator is then supplied with strong liquid NH_3-H_2O solution. A portion of the solution is evaporated by adding heat from a source to the solution. The vapor which is rich with NH_3 passes through a rectifier, which separates the water and sends it back to the generator. The pure NH_3 vapor at high pressure then proceeds through the other parts of the cycle. The weak solution exits the regenerator is throttled to the absorber pressure.

Heat transfer from an external source is the foundation for these systems' operation. For this reason, systems using absorption refrigeration are frequently categorized as heat-driven systems.

ARS is perfect for integration with solar thermal systems since it can use low-grade heat sources that would otherwise be squandered, which is one of its main advantages. For rural locations and impoverished nations where the availability of energy may be costly or unpredictable, this feature makes ARS a desirable option. Furthermore, ARS uses natural refrigerants that have zero or very little global warming potential (GWP) and zero ozone depletion potential (ODP), which helps to mitigate climate change and promote sustainable development. However, there are drawbacks to absorption refrigeration systems as well. They typically have a coefficient of performance (COP) of 0.5 to 0.7 for single-effect systems, which is lower than that of vapor compression systems. To maintain stable functioning, ARS also needs accurate temperature and pressure control, particularly in the absorber and generator. In addition, the systems need a bigger initial capital investment and are often heavier and bulkier than VCRS units. Improved heat exchangers, hybrid topologies that integrate compression and absorption technologies, and double-effect and triple-effect cycles are some of the recent developments that aim to increase the efficiency and compactness of ARS. With these advancements, ARS should become more practical and competitive for a wider range of applications.

1.7 Absorption-Compression Hybrid Refrigeration System

An absorption-compression hybrid refrigeration system combines elements of both absorption and compression refrigeration technologies to achieve improved efficiency or performance in certain applications. Both absorption and compression refrigeration systems are common methods for refrigeration, but they have their own advantages and disadvantages. Combining the advantages of both vapor compression and absorption refrigeration, the absorption-compression hybrid refrigeration system is an advanced refrigeration configuration that integrates the functionalities of both absorption and vapor compression refrigeration technologies. By integrating the advantages of each system, this hybrid strategy aims to overcome their specific shortcomings and improve operating flexibility, energy efficiency, and reliability especially in areas with fluctuating energy availability or high refrigeration demands.

When solar thermal energy or waste heat are available in sufficient amounts, which is usually during the day, they are employed to run the absorption cycle in a typical hybrid system. By using thermally powered processes to produce refrigeration, the absorption

component lessens reliance on electricity and greenhouse gas emissions. However, the system automatically transitions to a vapor compression cycle, which uses electrical energy to provide continuous cooling performance, when solar radiation is insufficient, such as at night, during cloudy weather, or during seasonal fluctuations. Because of its dual-mode operation, which guarantees constant refrigeration independent of thermal energy supply, it is ideal for crucial applications where temperature stability is crucial, like cold storage facilities, pharmaceutical preservation, and food processing. Regardless of the energy input source, the system can continuously reach the desired cooling temperature because of its capacity to adjust to available energy resources. In addition to ensuring refrigeration dependability, the integration of both systems may eventually result in cost and energy savings, particularly when renewable energy sources are used efficiently. Additionally, by lessening reliance on power during times of high demand, hybrid systems can help with peak load shaving.

However, there are difficulties in designing and putting into practice absorption-compression hybrid systems. These include the necessity for precise management strategies to handle the switching between operating modes and maintain energy efficiency, as well as increased system complexity and initial capital expenditure. To attain optimal performance, working fluids, system components, and thermal storage units must be carefully chosen.

The system contains the main absorption parts, in addition to the compressor which is connected in parallel with the absorber and generator as shown in the Figure 1.5.

Figure 1.5

Schematic of the proposed absorption-compression hybrid refrigeration cycle

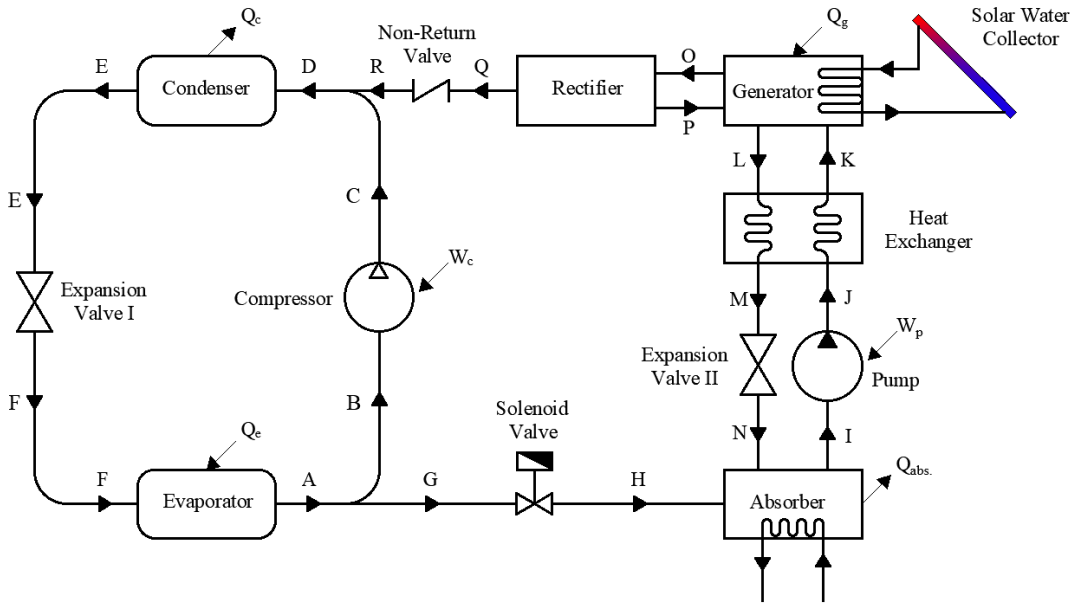

The generator, which uses a thermal energy source to separate the components of the strong solution into pure ammonia and water, is the central component of the hybrid refrigeration system. The main idea of the research is if it is possible to supply the generator with efficient thermal energy so that it can carry out its task. This is accomplished by using solar water heaters to heat the water that is supplied to the generator. Through a closed cycle, this water transfers its thermal energy to the generator's strong solution using a variety of heat transfer techniques. The temperature differential between the hot water and the potent solution within the generator is the cause of this. Scientific studies have indicated that the optimum water temperature for separating the strong solution inside the generator is 90 degrees Celsius, and therefore the study in this research was conducted based on that water temperature.

The operation principle of the absorption-compression hybrid refrigeration system depends of the generator inlet water temperature, if the temperature is less than 90 ℃ the system will work by vapor compression system, where the pure NH_3 refrigerant path will be B, C, D, E, F, and A. And if the inlet water temperature is greater than 90 ℃ the system will work by absorption, where the solenoid valve will energize to open and allowing the pure saturated vapor NH_3 to the passe through it, and the path will be G, H, (I, J, K), (L, M, N), (O, P), Q, R, D, E, F, and A. While the compression cycle is

running, the refrigerant won't be able to move from R to Q points because of the non-return valve. Hence, the purpose of the solenoid valve and the non-return valve is to control the working fluid's path in accordance with the current operating system.

1.8 Solar Water Heating Systems

The world's energy needs are rising dramatically as a result of industrial development and population expansion. To meet the needs of the world's expanding population, energy consumption is consequently rising quickly. One of the most significant forms of energy consumption is refrigeration and air conditioning, which is in high demand in hot climate countries due to rising internal thermal loads and increased consumer demand for thermal comfort. As a result, during the warmest summer days, the electrical power consumption of refrigeration equipment starts to produce issues in the supply network.

Solar water heating systems are renewable energy technologies designed to collect solar radiation to heat water for residential, commercial, and industrial applications. In addition to lowering energy costs and reducing reliance on fossil fuels, these systems also help to maintain environmental sustainability by minimizing greenhouse gas emissions.

Many advantages come with solar water heating systems: The abundance and renewable nature of solar energy makes it an environmentally friendly option for water heating. Energy cost savings, by utilizing solar energy, residences and commercial buildings may significantly reduce their reliance on fossil fuels, leading to lower energy expenses. Solar water heating produces far fewer greenhouse gas emissions than traditional water heating methods.

Evacuate tube collectors (ETC) absorbs heat from solar radiation and converts it into heat output which heats water flowing through the collectors. Convection and radiation losses are minimized by using the evacuated tube (Sharma, 2016).

The minimum generator temperature in an ammonia-water (NH_3-H_2O) absorption refrigeration system is a critical parameter that affects the overall performance of the system. In absorption refrigeration, the generator is a key component where heat is applied to separate the refrigerant (ammonia) from the absorbent (water). The minimum

generator temperature is the lowest temperature at which the absorption process can effectively take place, ensuring the separation of ammonia from water. This temperature is influenced by the specific design and operating conditions of the absorption refrigeration system. In practice, the minimum generator temperature for NH_3-H_2O absorption refrigeration systems is typically in the range of 70 to 90 degrees Celsius (158 to 194 degrees Fahrenheit). Operating the generator at temperatures below this range may result in incomplete separation of the refrigerant and absorbent, leading to reduced efficiency and performance of the refrigeration system. It's important to note that the exact minimum generator temperature can vary based on factors such as the concentration of the absorbent solution, pressure levels, and the specific design of the absorption system.

The COP has the higher values when using the input generator temperature with a minimum temperature of working of 111 and 109°C for absorption chiller Jesús Cerezo Román et al. (2019). The driving energy needed to bring the ammonia-water mixture to a boil is generated using a heating fluid that has a temperature range of 80 to 120 °C. For double-stage absorption cycles or compression-resorption cycles, lower driving agent temperatures from solar, geothermal, or waste heat sources can be employed (Hera & Vasilescu, 2011).

In order to attain optimal generator performance and efficiency and avoid water leakage from the generator to the condenser, the minimum inlet water temperature chosen for this research is 90 ℃.

Chapter Two

Methodology

2.1 Work Phases

A cold room model will be worked on, and it will be studied from the following three perspectives:

1. Vapor compression refrigeration system (VCRS). (Figure 1.3)
2. Absorption refrigeration system (ARS). (Figure 1.4)
3. Absorption-compression hybrid refrigeration system (ACHRS). (Figure 1.5)

Based on the steps and assumptions listed below:

1. The cold room cooling load is 3.5 kW
2. The working fluid for VCRS is ammonia (R717), and for the ARS is ammonia-water (NH3-H2O). Ammonia works as the refrigerant and water works as the absorbent.
3. Calculate the VCRS capacity of the refrigeration unit for the specified cold room, then analysis of its energy consumption and performance.
4. Calculate the ARS capacity of the refrigeration unit for the specified cold room, then analysis of its energy consumption and performance.
5. Selection of solar water heating system.
6. Based on the preceding processes, the capacity of the appropriate compressor and absorption refrigeration unit will be estimated and then will be studied as a combined unit. Then, during the year, an analysis of the new system's energy consumption and performance will be conducted.
7. Comparing and performing economic analysis for the three systems.
8. Obtain the results

2.2 Modeling of the Vapor Compression Refrigeration System (VCRS)

Applying the second law of thermodynamics to the main components of the vapor compression refrigeration system as shown in the Figure 1.3 which are compressor, condenser, expansion valve, and the evaporator.

The ammonia refrigerant mass flow rate will be the same in each part of the cycle, and indicated by $\dot{m}_r$.

2.2.1 Compressor

The saturated vapor ammonia enters the compressor in low pressure and low temperature at point 1, and leaves it in superheated phase with high pressure and high temperature at point 2 in isentropic process, as shown in the Figure A.4 in Appendix A.

By applying the energy balance at the compressor:

$$W_C = \dot{m}_r \, (h_2 - h_1) \tag{1}$$

Where:

W_C is the compressor work done in [kW],

$\dot{m}_r$ is the refrigerant flow rate in [kg\s],

h_1 is the refrigerant enthalpy in the compressor suction line in [kJ/kg],

h_2 is the refrigerant enthalpy in the compressor discharge line in [kJ/kg].

2.2.2 Condenser

The superheated vapor condensed in the condenser in isobaric process, by rejecting the heat to the surrounding, the high-pressure saturated liquid pure ammonia leaves the condenser at pint 10, as shown in the Figure A.5 in Appendix A.

By applying the energy balance at the condenser:

$$Q_c = \dot{m}_r \, (h_3 - h_2) \tag{2}$$

Where:

Q_c is the condenser load in [kW],

h_3 is the refrigerant enthalpy which leaving the condenser in [kJ/kg].

2.2.3 Expansion Valve

The high-pressure saturated liquid ammonia enters the expansion valve to reduce its pressure in adiabatic process, therefore low-pressure ammonia refrigerant leaves it in mixture phase at point 4, as shown in the Figure A.6 in Appendix A.

So, the energy balance at the expansion valve will be:

$$h_3 = h_2 \tag{3}$$

Where:

h_3 is the enthalpy for refrigerant leaving the expansion valve in [kJ/kg].

2.2.4 Evaporator

The low-pressure mixture refrigerant evaporates in the evaporator in isobaric process, by absorbing heat from the refrigerated space, and leaves it in low pressure saturated vapor at point 1 and 4 respectively, as shown in the Figure A.7 in Appendix A.

By applying the energy balance at the evaporator:

$$Q_e = \dot{m}_r \, (h_1 - h_4) \tag{4}$$

Where:

Q_e is the evaporator load, also known as the cooling load in [kW],

h_4 is the refrigerant enthalpy which entering the evaporator in [kJ/kg].

so, the refrigerant flow rate can be calculated as:

$$\dot{m}_r = \frac{Q_e}{(h_1 - h_4)} \tag{5}$$

h_1 and h_4 can be taken from the P-h diagram for R717 refrigerant (Appendix B).

2.2.5 VCRS Coefficient of Performance (COP)

COP is defined as the relationship between the useful cooling capacity in kW to the power in kW that is supplied to the compressor.

$$COP = \frac{Evaporator\ Capcity\ in\ (kW)}{Compressor\ Work\ (kW)} \tag{6}$$

2.2.6 VCRS Load Analysis

Load analysis can be performed manually by taking enthalpy values from the P-h diagram for R717 refrigerant, and substituting them into the above equations. Calculations can also be performed using special software's such as CoolPack, and engineering equation solver (EES). In this research, the calculations were performed using both of the mentioned software's, and the results were identical, noting a slight discrepancy that can be neglected.

In this research, the cooling load and temperatures will be considered for both the evaporator and the condenser are 3.5 kW, 0℃, and 45℃ respectively. Considering the following presumptions while performing a thermodynamic analysis of the VCRS:

1. The refrigerant is in low pressure saturated vapor at point 1.
2. The refrigerant is in high pressure superheated vapor at point 2.
3. The refrigerant is in high pressure saturated liquid at point 3.
4. The refrigerant is in low pressure mixture at point 4.

The compressor work, the capacities of the evaporator and condenser, and COP are calculated by CoolPack software based on the temperatures of the evaporator and condenser, and the cooling load. The Figure A.11 in Appendix A indicated to the CoolPack software window, and the P-h diagram for R717 refrigerant at this case illustrated in the Appendix B.

EES is a software tool used for solving and modeling thermodynamic and fluid flow problems. It's commonly employed in engineering disciplines for analyzing and solving complex systems involving energy and mass transfer. EES is considered more complex than the CoolPack software because data must be entered using a particular programming language. A major feature of EES is the high accuracy thermodynamic and transport property database that is provided for hundreds of substances in a manner that allows it to be used with the equation solving capability. Figures A.9 and A.10 in Appendix A shows the refrigeration cycle in EES window, and the properties of each state based on evaporator, and condenser input temperatures, and the required cooling load.

Consequently, the required VCRS as follows, using EES software:

- The evaporator capacity = 3.5 kW
- The condenser capacity = 4.195 kW
- The compressor work = 0.6949 kW
- The coefficient of performance (COP) = 5.037

2.3 Modeling of the Absorption Refrigeration System (ARS)

Applying the second law of thermodynamics to the main components of the ARS as shown in the Figure 1.4, the following presumptions are taken into account while performing a thermodynamic analysis of each component of the ARS:

1. At points 1, 4, and 10, the phase is saturated liquid.
2. At point 12, there is a pure ammonia in saturated vapor phase.
3. At point 10, there is a pure ammonia in saturated liquid phase.
4. At point 9, there is a pure ammonia in superheated vapor phase.
5. There are two pressure limits, low pressure and high pressure, evaporator and absorber as well as generator and condenser are under the same pressure limits.
6. Low pressure (P_L) = P_1 = P_6 = P_{11} = P_{12}

7. High pressure (P_H) = P_2 = P_3 = P_4 = P_5 = P_7 = P_8 = P_9 = P_{10}

8. Flow at the throttling devices is adiabatic.

9. Pumping is isentropic process.

10. Strong solution represented with the points 1, 2, and 3. The percentage of the strong solution at these points will remain the same.

11. Weak solution represented with the points 4, 5, and 6. The percentage of the weak solution at these points will remain the same.

12. Pure ammonia flow rate ($\dot{m}_r$) at the condenser, expansion valve I, and the evaporator are the same as in VCRS, therefore $\dot{m}_r = \dot{m}_9 = \dot{m}_{10} = \dot{m}_{11} = \dot{m}_{12}$

13. The concentrations at points 8 and 3 are the same.

2.3.1 Generator

The strong solution is supplied to the generator with mass flow rate $\dot{m}_{ss}$, concentration X_{ss}, and temperature T_3, as shown in the figure in Appendix B.8.

The weak solution leaves the generator with mass flow rate $\dot{m}_{ws}$, concentration X_{ws}, and temperature T_4. Superheated solution leaves the generator with mass flow rate $\dot{m}_7$, concentration X_7, and temperature T_7, and water return to the generator with mass flow rate $\dot{m}_8$, concentration X_8, and temperature T_8. The generator's heating medium enters at point 13. The generator load can be calculated by applying the energy and mass balance at the generator.

Energy balance at the generator:

$$Q_G + \dot{m}_{ss} h_{ss} + \dot{m}_8 h_8 = \dot{m}_7 h_7 + \dot{m}_{ws} h_{ws} \quad (7)$$

Where:

Q_G is the generator load in [kW],

h_{ss} is the strong solution enthalpy in [kJ/kg],

h_{ws} is the weak solution enthalpy in [kJ/kg].

Mass balance at the generator:

$$\dot{m}_{ss}X_{ss} + \dot{m}_8X_8 = \dot{m}_{ws}X_{ws} + \dot{m}_7X_7 \quad (8)$$

2.3.2 Rectifier

The pure ammonia in superheated vapor phase leaves the rectifier with mass flow rate $\dot{m}_9$, and temperature $T_{9,}$ as shown in the Figure A.12 in Appendix A. To find the rectifier load, energy and mass balance will be applied.

Energy balance at the rectifier:

$$\dot{m}_7h_7 = \dot{m}_8h_8 + \dot{m}_9h_9 + Q_{rec} \quad (9)$$

Where:

Q_{rec} is the rectifier load in [kW],

h_7 is the superheated vapor solution enthalpy entering the rectifier in [kJ/kg],

h_8 is the water vapor enthalpy leaves the rectifier in [kJ/kg],

h_9 is the pure ammonia in superheated vapor enthalpy in [kJ/kg].

Mass balance at the rectifier:

$$\dot{m}_7X_7 = \dot{m}_8X_8 + \dot{m}_9 \quad (10)$$

2.3.3 Condenser, Expansion Valve I, and the Evaporator

The procedure is the same as in VCRS. Where the condenser, expansion valve I, and the evaporator properties are the same. Therefore:

- Point 2 is the same of point 9
- Point 3 is the same of point 10
- Point 4 is the same of point 11
- Point 1 is the same of point 12

2.3.4 Absorber

Pure saturated vapor ammonia enters the absorber at a rate of $\dot{m}_{12}$, weak solution enters to the absorber at a rate of $\dot{m}_{ws}$ and concentration X_{ws}, as shown in Figure A.13 in Appendix A. Strong solution leaves the absorber with a flow rate $\dot{m}_{ss}$ and concentration X_{ss}. Cooling agent inters the absorber from point 15 and leaves the absorber at point 16.

The absorber load can be calculated by applying the energy and mass balance at the absorber.

Energy balance at the absorber:

$$\dot{m}_{12}h_{12} + \dot{m}_{ws}h_{ws} = Q_a + \dot{m}_{ss}h_{ss} \tag{11}$$

Where:

Q_a is the absorber load in [kW],

h_{12} is the saturated vapor ammonia enthalpy entering the absorber in [kJ/kg].

Mass balance at the absorber:

$$\dot{m}_r + \dot{m}_{ws}X_{ws} = \dot{m}_{ss}X_{ss} \tag{12}$$

2.3.5 Heat Exchanger

Strong solution at flow rate $\dot{m}_{ss}$ is heated from T_2 to T_3, and weak solution at flow rate $\dot{m}_{ws}$ is cooled down from T_4 to T_5 as shown in the Figure A.14 in Appendix A.

Assume the heat exchanger efficiency is 1, so the heat exchanger load calculated by applying the energy and mass balance at the heat exchanger.

Energy balance at the heat exchanger:

$$\dot{m}_{ss}(T_3 - T_2) = \dot{m}_{ws}(T_5 - T_4) \tag{13}$$

Mass balance at the heat exchanger:

$$\dot{m}_{ss}X_{ss} + \dot{m}_{ws}X_{ws} = \dot{m}_{ss}X_{ss} + \dot{m}_{ws}X_{ws} \quad (14)$$

2.3.6 Pump and Expansion Valve II

EES software will calculate the pump and expansion valve II since they are not significant to the study, and can be computed using the same way as before.

2.3.7 ARS Coefficient of Performance (COP)

The COP of ARS is defined as the relationship between the desired output to the required input, where the required input is the thermal generation heat source, and the pump work, but the pump work is can be negligible since it's too small.

$$COP_{ARS} = \frac{Desired\ output}{Required\ input} = \frac{Q_e}{Q_G} \quad (15)$$

2.3.8 ARS Load Analysis

Since absorption refrigeration system calculations are thought to be rather complex, EES software was used to carry out the calculations and establish the loads for each system component, EES supports a wide range of thermodynamic and transport property functions, making it suitable for modeling complex systems. To perform calculations for an ARS using EES software, the general procedures that need to be followed are as follows:

1. Defining the working fluid and identifying the parts of the absorption refrigeration system.

2. Define variables, parameters, and equations that represent the thermodynamic processes occurring in each component of the system.

3. Input the known data such as temperatures, pressures, and concentrations.

4. Express the thermodynamic equations that govern the behavior of the absorption refrigeration system, including the equations for energy and mass balances.

5. Checking the equations, solving them, and extracting the results.

Appendix C shows how the EES program was used to write all of the ARS properties, and equations that needed to be solved. The Figure A.15 in Appendix A shows the thermodynamic properties of each state in the ARS by EES software.

The points in the Figure A.15 in Appendix A differ from the points shown in the absorption refrigeration cycle schematic in Figure 1.2, as the point 10 corresponds to point 11 in EES, point 11 corresponds to point 12, and point 12 corresponds to point 14 as well. The heat exchanger on the mechanical cycle side is represented by points 11 and 13 in the EES table, and it can be disregarded.

The negative sign in enthalpy relates to the direction in the simulation, not the value

After solving the equations by EES software, the results for the ARS component's capacities are illustrated in Figure 2.1.

Figure 2.1

ARS capacities by EES software

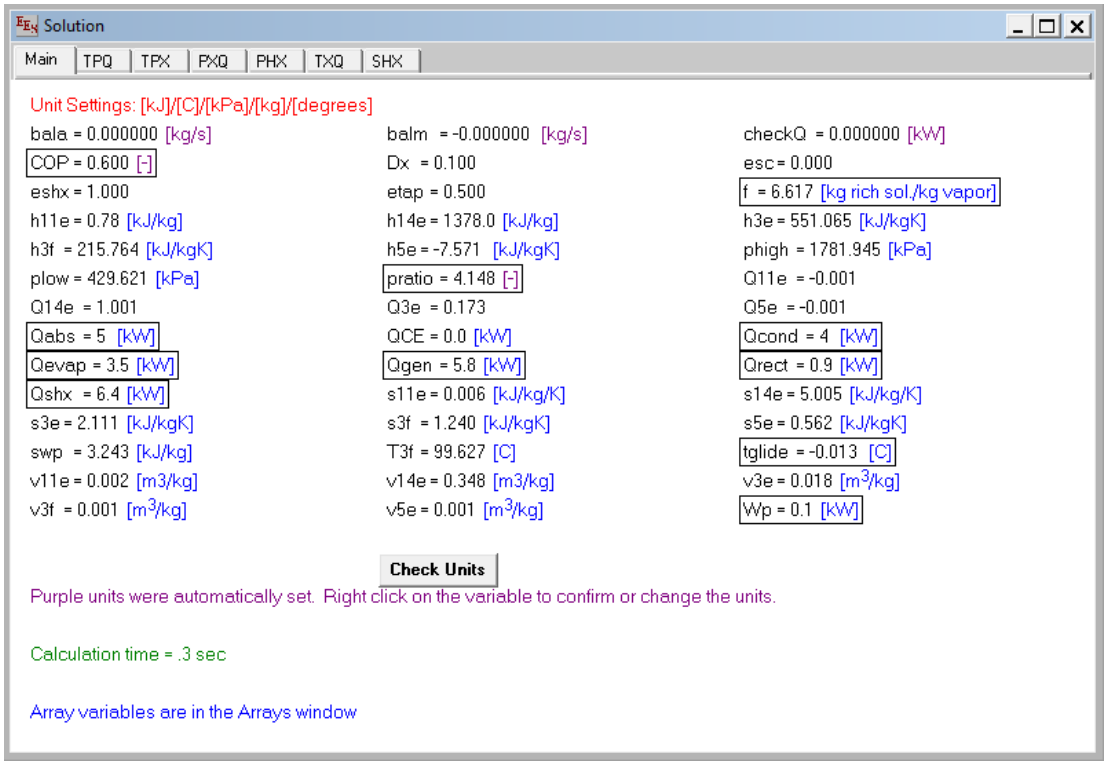

Consequently, the required ARS as follows, using EES software:

- The generator capacity = 5.8 kW
- The rectifier capacity = 0.9 kW
- The condenser capacity = 4.0 kW, same as VCRS, having an insignificant variation that is overlookable.
- The evaporator capacity = 3.5 kW, same as VCRS.
- The absorber capacity = 5.0 kW
- The heat exchanger capacity = 6.4 kW
- The pump work = 0.1 kW
- The coefficient of performance (COP) = 0.6

2.4 Modeling of the Solar Water Heating System

Climate and sunlight conditions, collector efficiency, orientation and tilt, collector material, absorption coating, tube design, vacuum quality, and cost considerations, are things that must be taken into account while choosing evacuated tube solar water collectors (ETC) to guarantee maximum effectiveness and performance.

In this study, ETC was selected for water heating. The selection process was carried out using SAM software in accordance with the 5.8 kW generator capacity that was computed in the ARS. The ETC water flow rate must first be known, this can be assumed by the ETC technical data sheet as shown in Figure A.16 in Appendix A.

The ETC type HP30-3000 was selected. The aperture area, efficiency, and flow rate parameters are utilized in SAM software to know the output temperature of the water from ETC.

Considering the global horizontal solar radiation and the ambient air-dry bulb temperature most recent available data from the NSRDB, the useful solar energy can be calculated by the equation (16).

$$Q_u = \eta_c \times G \times A_c \quad (16)$$

Where:

Q_u is the useful energy absorbed by the collector in [kW],

η_c is the collector's efficiency,

G is the global horizontal solar radiation in [kW/m^2],

A_c is the collector area in [m^2].

Then, the output water temperature from ETC can be calculated by equation (17).

$$T_{w,o} = \frac{Q_u}{\dot{m}_w \times cp_w} + T_{w,i} \quad (17)$$

Where:

$T_{w,o}$ is the output water temperature from ETC in [°C],

$T_{w,i}$ is the input water temperature to the ETC in [°C],

$\dot{m}_w$ is the ETC water flow rate in [kg\s],

cp_w is the specific heat capacity of water in [kJ\kg. °C].

Modeling was conducted using SAM software, and it was found that the system needed three solar collectors' type HP30-3000. and the hourly useful energy will be around the generator's capacity (5.8 kW) from May to September months, as shown in Figure 2.2.

Figure 2.2

Hourly useful energy

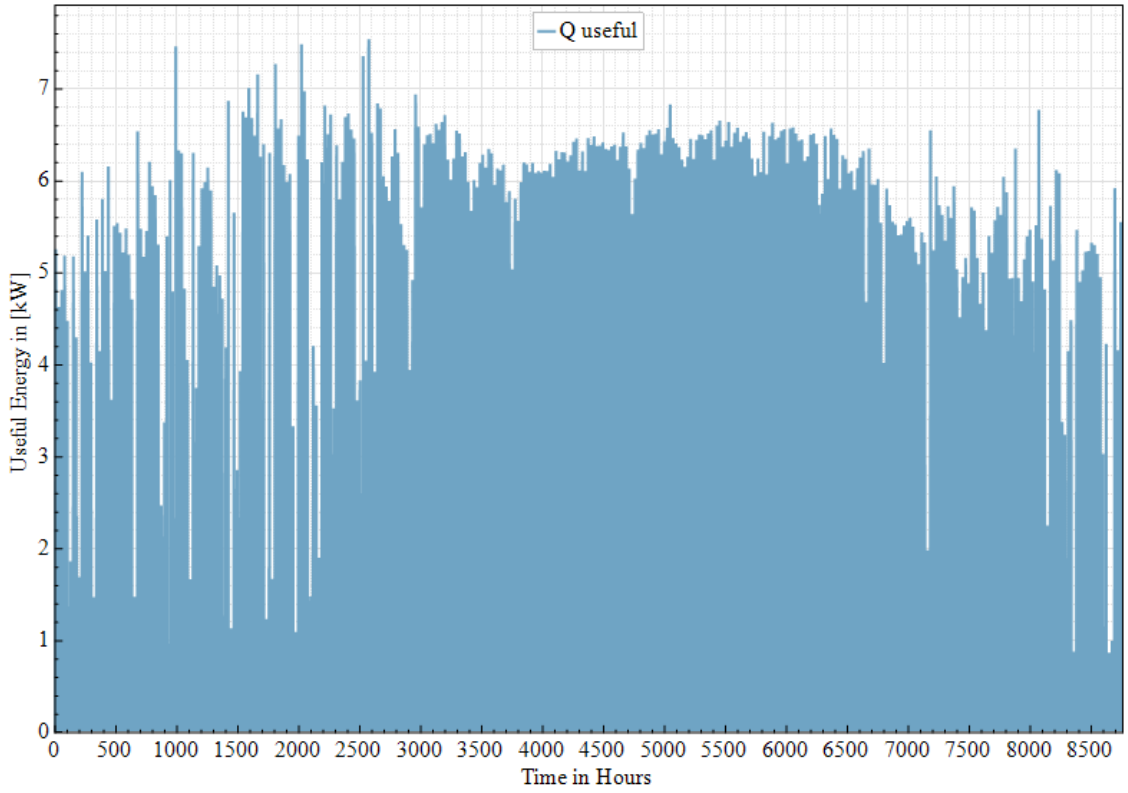

Figure 2.3 shows the amount of utility energy used per hour to get water over 90 degrees Celsius, around the year. The required energy in the range of 4.6 to 6.7 kW. Because the water retains its energy and stays warmer than the outside air temperature, less energy is needed to heat it and get it to the proper temperature the next day. This is the reason the energy required is less than the generator capacity. The temperature of the water generated by the solar water heating system and the ambient temperature at each hour of the year are displayed in Figure 2.4. The system has a total operating capacity of 2078 hours a year, which constitutes 24% of the number of hours per year.

Figure 2.3

The amount of utility energy used per hour to get water over 90 degrees Celsius

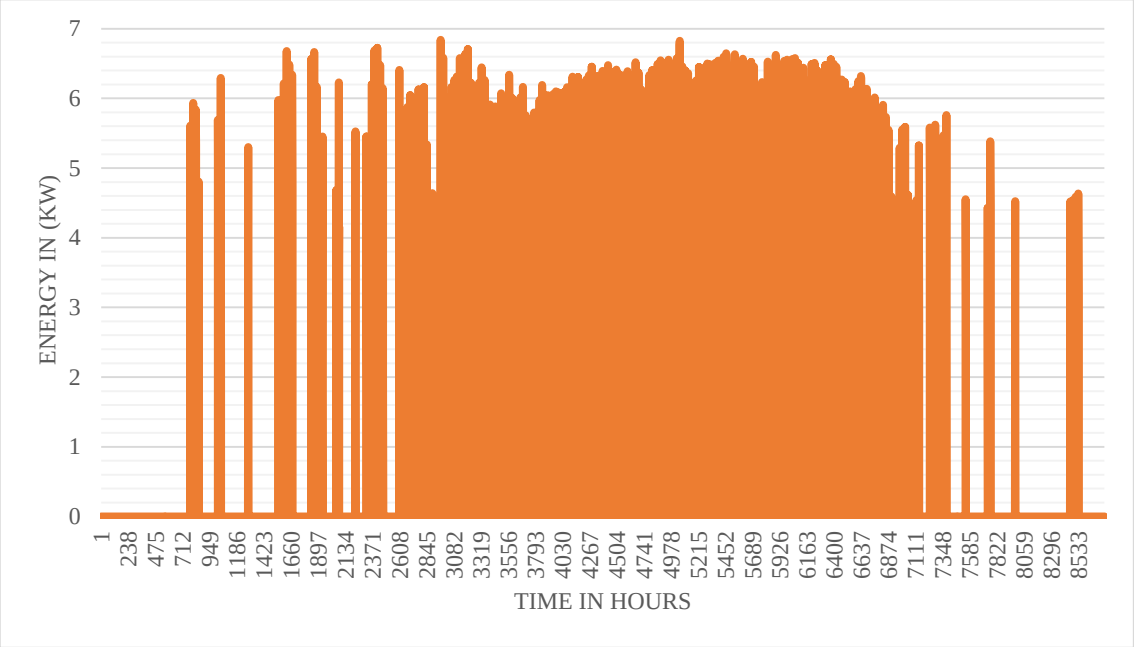

Figure 2. 4

The annual delivered water temperature by the solar water heating system and the ambient temperature

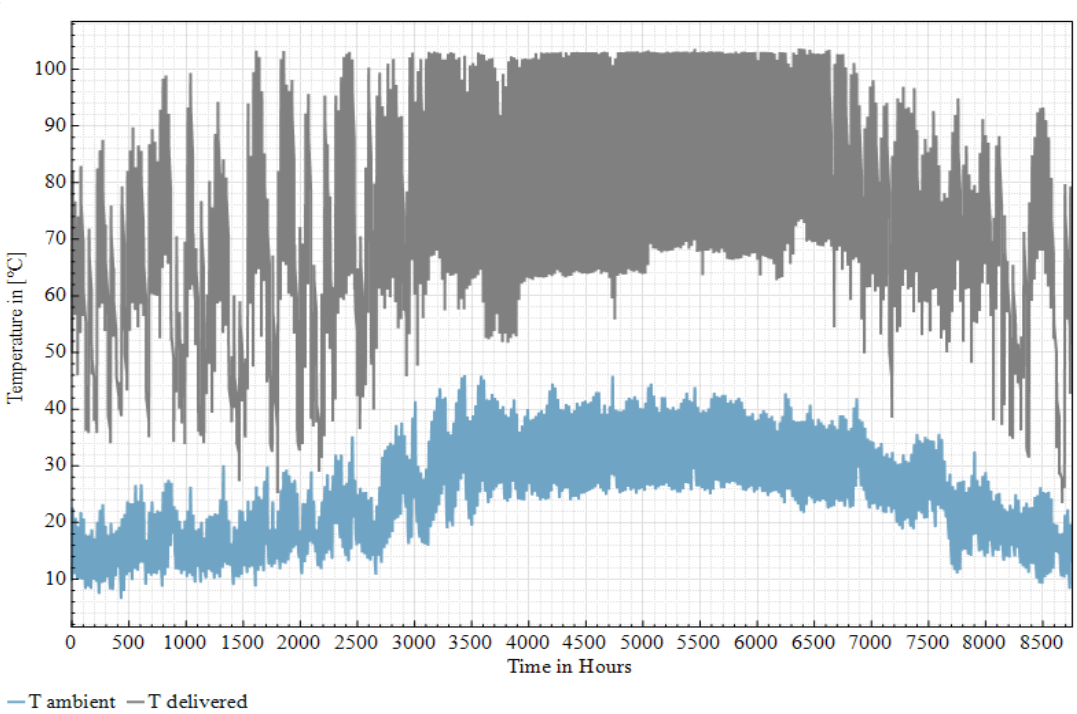

A full year's worth of hourly variations in the ambient air temperature and the water temperature delivered by the solar water heating system are shown in Figure 2.4. Temperature in degrees Celsius (℃) is displayed on the y-axis, while time is represented on the x-axis in hours (0–8760). In reaction to seasonal variations in the ambient temperature, the plot offers a comparative evaluation of the system's thermal performance. The output temperature stays far over 90℃ throughout the majority of the late spring, summer, and early fall months (about from hour 3000 to 7000), and the delivered water temperature (shown in grey) continuously surpasses the ambient temperature (shown in blue) throughout the year. The evacuated tube solar collectors perform better during this time due to increased solar irradiance and better ambient conditions. The output temperature fluctuates more throughout the winter months (early and late in the year), sometimes dropping below the desired threshold. This tendency is a result of lower ambient temperatures and less available solar energy. However, the system has efficient solar gathering and thermal storage capabilities, maintaining adequate output for a significant portion of the year. With peaks exceeding 40℃ in the summer and below 10℃ in the winter, the ambient temperature curve exhibits a typical seasonal pattern. The system's capacity to continuously raise water temperature substantially above ambient settings, especially when solar energy is plentiful, is demonstrated by the notable difference between delivered and ambient temperatures, despite the variations.

2.5 Modeling of the Absorption-Compression Hybrid Refrigeration System (ACHRS)

Component capacities of the ACHRS are assumed in the previous two sections. The generator's water inlet temperature is crucial to the ACHRS's functionality. The key to solving this problem is to take into account the solar energy that produces the necessary hot water temperature since the generator load has already been determined.

Merging the VCRS and ARS together is the core of this research. If the output water temperature from the solar water collector is sufficient, the system will operate by ARS, else by VCRS. Therefore, knowing the period of operation of ARS depends on weather data in Jericho, and the ambient temperatures for each hour around the year.

The analysis done for both systems, VCRS, and ARS, as the result, the VCRS can operate around the year with work 0.649 kW, and the ARS can operate efficiently by solar energy 2078 hours around the year, with 24% from the total hours in the year. But ARS can’t operate efficiently in the rest of the hours around the year.

The working principle of the ACHRS was explained on chapter 1, section 9, and the cycle schematic shown in Figure 1.3. The system will operate by VCR 6682 hours per year and by ARS 2078 hours per year as shown in Figure A.17 in Appendix A. As a result, the system starts off using vapor compression and needs to be switched to the absorption system as soon as the output water generator entering the system reaches the proper temperature. It is vital to include a temperature controller in order to make sure that the refrigerator is operating with absorption at the proper temperature. The system is ensured to operate well and consume less energy in this manner.

2.6 Economic Analysis

In general, absorption refrigeration systems are used to lower energy costs and lessen the damaging effects of greenhouse gas emissions on the environment. Thermodynamic analysis and optimization are methods of increasing efficiency in refrigeration systems, and studies on this topic have expanded recently.

As a result of the compressor's need for electricity to increase the refrigerant's pressure, the VCRS is referred to as a work-operated cycle. In contrast, ARS is sometimes known as a heat-operated cycle since the majority of its running costs are incurred in producing the heat necessary to remove the vapor refrigerant from the generator's high-pressure liquid solution. While some electricity is needed to run the pump in the absorption cycle, it is not as much as it is in the vapor compression refrigeration cycle for a given amount of refrigeration.

An economic feasibility study was made for operating the refrigeration system by VCRS, and ACHRS. ARS wasn't considered because it is ineffective for year-round operation. A Simple Payback Period (SPP), Net Present Value (NPV), and Internal Rate of Return (IRR) are methods of economic analysis used in this research to assess the feasibility of the two mentioned scenarios.

SPP offers a rapid evaluation based on payback time, whereas NPV and IRR offer a more thorough analysis that takes the time value of money into account. While IRR determines the discount rate at which the net present value (NPV) is zero, NPV compares the present value of cash inflows and outflows. When making well-informed financial decisions, all three approaches are employed.

The economic analysis was conducted according to the three systems costs shown in Table 2.1, as well as the energy tariff price is 0.22 US dollars. Table 2.2 shows the annual energy cost by operating VCRS, and ACHRS considering the number of hours that ARS can operate. Typically, the cold storage refrigeration system runs daily for around 16 hours out of 24 because the thermostat shuts off the compressor when the proper temperature is reached.

Table 2.1

The costs of the three systems

	Unit Price (USD)	ETC (USD)	Control System (USD)	Life Time (Yr.)
VCRS	550	-	-	15
ARS	260	800	-	-
ACHRS	810	800	135	20

Table 2.2

The annual energy cost by operating VCRS, and ACHRS systems

	Input Power (kW)	Daily Operating Ratio (%)	Annual Operating Hours (hr/Yr.)	Tariff Cost (USD/kWh)	Annual Energy Cost (USD\Yr.)
VCRS	0.6949	67	8760	0.22	892.808
ACHRS	0.6949	67	6682	0.22	681.021
Savings	0.6949	67	2078	0.22	211.787

2.6.1 Simple Payback Period

One of the most popular techniques for assessing the financial viability of an investment is the Simple Payback Period (SPP), especially when it comes to energy systems like solar-powered refrigeration, absorption refrigeration, or hybrid energy technologies. Usually stated in years, it computes the period in years that an investment must provide net cash inflows to recoup its initial cost. Put otherwise, it's the amount of time it takes for a project's total revenues or cost savings to match its initial capital expenditure.

Generally, a shorter payback period is considered more feasible, as it indicates a quicker return on investment.

The formula for calculating the SPP is:

$$SPP = \frac{Investment}{Savings} \tag{18}$$

The investment cost is the summation of the ARS, ETC, and ACHRS control system costs, while the savings cost is the difference between the annual energy costs of the VCRS, and ACHRS.

The feasibility of installing solar thermal-driven refrigeration systems in places like Jericho, where there is a high need for cooling and a high level of solar radiation, is evaluated in this study using the Simple Payback Period. Over time, switching to hybrid or absorption-based systems can result in significant cost savings because traditional vapor compression refrigeration systems use a lot of electricity, particularly in hot areas. SPP calculations assist policymakers, cold storage operators, and farmers in understanding return on investment and making well-informed financial decisions.

2.6.2 Net Present Value

A more advanced measure that accounts for the time value of money is called net present value (NPV). It deducts the initial investment and reduces future cash flows to their present value. An investment with a positive NPV will be feasible. By acknowledging that a unit of currency today has greater earning potential than the same amount in the future, it takes into consideration the temporal value of money. The project is deemed financially attractive if the net present value is positive, meaning that over time, the anticipated revenue or savings will surpass the initial investment and cost. The project would result in a net loss if the NPV was negative, making it unwise from a financial standpoint.

The formula for calculating the NPV is:

$$NPV = \sum_{t=0}^{T} \frac{CF_t}{(1+r)^t} - C_0 \tag{19}$$

Where:

T is the number of periods,

CF_t is the net cash flow during the period t,

r is the rate of return required for the investment,

C_0 is the initial investment cost.

The total period considered is 20 years which is the ACHRS lifetime.

The long-term financial benefits of implementing ACHRS are assessed in this study using net present value (NPV) in contrast to conventional vapor compression systems. The NPV technique aids in capturing the overall economic value during the system's operational life, which is normally 15 to 25 years, because these systems frequently have a high upfront cost but lower operating expenses. For example, in a hot area like Jericho, installing a solar-powered absorption system can drastically save yearly electricity costs, particularly during the best refrigeration months. Even if the initial outlay could be greater than for a traditional system, the NPV analysis shows if the savings over time outweigh the expense. A key factor in NPV computations is the selection of the discount rate. Projects appear less profitable when the discount rate is larger because it lowers the present value of future savings, whereas a lower rate has the reverse effect.

2.6.3 Internal Rate of Return

An important financial indicator for assessing an investment's profitability is the Internal Rate of Return (IRR), which calculates the discount rate at which the Net Present Value (NPV) of all cash flows both income and costs becomes zero. The estimated yearly percentage return that the project is expected to generate over its lifetime is known as the internal rate of return. The Internal Rate of Return (IRR), also

referred to as the discount rate, is what reduces the net present value of an investment to zero. The anticipated annualized rate of return on investment is displayed. If the IRR is higher than the required rate of return, the project is considered acceptable.

Mathematically, the IRR can be found by solving the following equation:

$$\sum_{t=0}^{T} \frac{CF_t}{(1+IRR)^t} - C_0 = 0 \tag{20}$$

A project is considered financially viable if the IRR exceeds either the minimum acceptable rate of return or the cost of capital. On the other hand, the investment would not be appealing if the IRR were less than the cost of capital. The economic viability of building ACHRS is assessed in this study using internal rate of return (IRR). Because these systems use renewable energy sources (such solar thermal energy) rather of electricity-driven compression, they typically have higher initial capital expenditures but lower operational costs.

Chapter Three

Results

3.1 Introduction

This chapter summarizes the findings of a comparative study of three refrigeration systems: the Absorption Refrigeration System (ARS), the Vapor Compression Refrigeration System (VCRS), and the Absorption-Compression Hybrid Refrigeration System (ACHRS). A 3.5 kW thermal load was applied to a cold storage facility in order to evaluate each system's performance, operational viability, and economic feasibility.

3.2 Performance of Individual Refrigeration Systems

3.2.1 Vapor Compression Refrigeration System (VCRS)

The VCRS operates entirely on electrical energy, with the compressor being the primary consumer of power. The system is capable of operating throughout the entire year, offering continuous refrigeration with a coefficient of performance (COP) of approximately 5. This system provides reliable performance independent of solar availability, though it is associated with high energy consumption due to the mechanical work required by the compressor.

3.2.2 Absorption Refrigeration System (ARS)

The ARS, on the other hand, uses solar thermal energy to heat water to 90°C or more, which is required to power the absorption cycle. This temperature threshold was only reached for 2,078 hours a year, or roughly 24% of the 8,760 hours of total annual hours, according to data on local solar radiation. The ARS's standalone practicality for cold storage applications in the examined region is thus limited by its inability to function year-round.

3.2.3 Performance of the Hybrid System (ACHRS)

A hybrid configuration (ACHRS) that integrates ARS and VCRS was created in order to overcome the constraints of ARS and VCRS. Combining the ARS and VCRS, the ACHRS uses the VCRS when there is insufficient solar input and the ARS when there

is enough solar availability. Under this arrangement, the ARS operates 2,078 hours annually (24%), and the VCRS operates 6,682 hours annually (76%). Based on current electricity rates, this operating method saved 962.668 kWh of energy annually, which translates to a cost savings of 211.787 USD.

3.3 Evaluation of economic outcomes

Economic analysis was conducted to determine the viability of the ACHRS. The SPP is 5.6 years, indicating that the investment will need 5.6 years to generate enough cash flows to cover its initial cost. On the other hand, NCF is 637.811 USD, which is considered economically feasible, Figure 3.1 shows the cash flow chart for ACHRS. Furthermore, an IRR is 17% indicates the feasibility of the system because IRR exceeds the rate of return (10%).

Figure 3.1

Cash flow chart for ACHRS

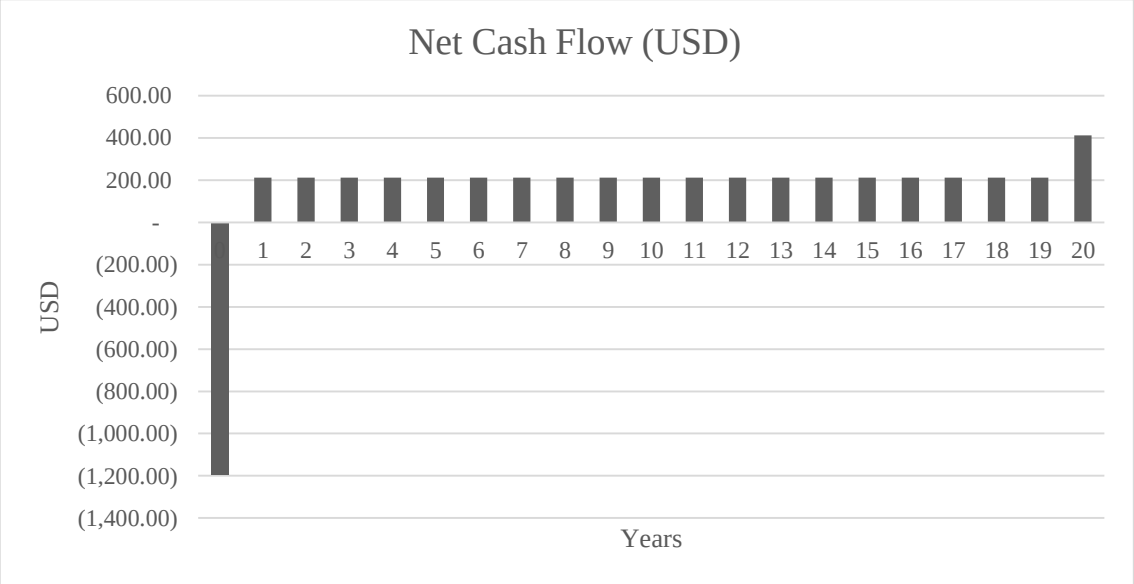

3.4 Summary of Results

The results show that the VCRS has substantial energy expenditures even though it guarantees year-round operation. Even though the ARS uses less energy when the sun is shining, its limited sunlight availability makes it unsuitable as a stand-alone device. The benefits of both systems are successfully combined in the ACHRS, which shows up as a reasonable and workable option. It confirms its potential as a sustainable solution for cold storage applications by providing significant energy and cost savings, as well as positive economic indicators like a quick payback period and strong internal rate of return.

Chapter Four

Conclusion and Recommendations

4.1 Conclusion

One of the most notable advantages of absorption refrigeration systems (ARS) over vapor-compression refrigeration systems (VCRS) lies in the type of compression involved in the thermodynamic cycle. In ARS, compression is applied to a liquid solution rather than a vapor. Since the work input in steady-flow processes is directly proportional to the specific volume of the fluid, and liquids have a significantly lower specific volume than gases, the mechanical work required in ARS is minimal typically around 1% of the thermal energy supplied to the generator. This small mechanical input is often considered negligible in cycle analysis, making absorption systems highly attractive for applications where low-grade thermal energy is available, such as solar thermal or waste heat sources.

An economic and performance comparison is often made between these two refrigeration technologies: vapor compression refrigeration system (VCRS) powered by electrical energy and a vapor absorption refrigeration system (ARS) powered by solar evacuated tubes unit. The comparison is generally based on key factors such as energy efficiency (COP), operating cost, and payback period.

While VCRS typically achieves higher coefficients of performance (COP), they are heavily dependent on electrical power and often use synthetic refrigerants with negative environmental impacts. In contrast, absorption systems can operate using natural refrigerants (such as ammonia or water) and renewable thermal energy, reducing operational emissions and long-term electricity costs. However, this comes with trade-offs.

Absorption refrigeration system is often more capital-intensive than their compression-based counterparts. They are typically larger in size, mechanically more complex, and less familiar to most service technicians, which can increase maintenance challenges and initial setup costs. Moreover, they are less efficient in terms of immediate refrigeration performance, especially under varying load conditions.

As a result, ARS should only be considered economically viable in scenarios where thermal energy is available at a low or zero cost for example, in facilities with abundant solar radiation or industrial waste heat and where electricity costs are high or access is limited. In such contexts, especially in off-grid or remote regions, solar-assisted absorption systems can offer long-term cost savings, energy independence, and environmental benefits, making them a compelling alternative despite the initial investment.

4.2 Recommendations

The Absorption-Compression Hybrid Refrigeration System (ACHRS) should be used for cold storage applications, especially in areas like Jericho that have high ambient temperatures, according to the study's findings. Because of the significant temperature difference between the refrigerated space and the outside environment, the higher refrigeration need in these regions leads to higher energy usage. Heat gain is accelerated by this scenario, making an economical and effective refrigeration system necessary.

By using solar thermal energy to run the absorption unit when there is enough solar radiation, the hybrid system successfully overcomes this difficulty and lessens reliance on electrical energy. To guarantee ongoing functioning during times of limited solar availability, the system transitions to the vapor compression unit. According to the study, this dual-mode flexibility not only guarantees operational dependability all year long but also significantly reduces energy consumption and enhances cost-effectiveness.

Furthermore, Jericho is a perfect place to install solar-assisted systems because to its high levels of sun irradiation. The study's economic analysis supported ACHRS's financial sustainability, citing positive metrics such a strong internal rate of return and a fair payback period.

Additionally, it is advised that the ACHRS be applied to cold storage facilities with thermal loads greater than those examined in this study in future research and implementation initiatives. Larger-scale systems are probably going to save more energy and have a more noticeable economic impact, which will produce more accurate and broadly applicable results. Long-term performance monitoring in real-world field settings is also advised in order to confirm the system's operational effectiveness and financial return.

List of Abbreviations

Abbreviation	Meaning
ACHRS	Absorption-Compression Hybrid Refrigeration System
VCRS	Vapor Compression Refrigeration System
ARS	Absorption Refrigeration System
NCF	Net Cash Flow
SPP	Simple Payback Period
NPV	Net Present Value
IRR	Internal Rate of Return
CFCs	Chlorofluorocarbons
HCFC	Hydrochlorofluorocarbons
GWP	Global Warming Potential
ODP	Ozone Depletion Potential
COP	Coefficient of Performance
NSRDB	The National Solar Radiation Data Base
NREL	National Renewable Energy Laboratory
SAM	System Advisor Model
NH_3	Ammonia
ASHRAE	American Society of Heating, Refrigerating and Air-Conditioning Engineers
ETC	Evacuate tube collectors
℃	Degrees Celsius
EES	Engineering Equation Solver

References

Abd, {m, Hamed, E., Mostafa, A., & Fatouh}, M. (2017). *Simulation of a Cold Store Driven by Solar Absorption Cooling System under Different Egyptian Climatic Conditions*.

Agyenim, F. B. (2007). *The development of medium temperature thermal energy storage for cooling applications*.

Balaras, C. A., Grossman, G., Henning, H. M., Infante Ferreira, C. A., Podesser, E., Wang, L., & Wiemken, E. (2007). Solar air conditioning in Europe—an overview. *Renewable and Sustainable Energy Reviews*, *11*(2), 299–314. https://doi.org/10.1016/J.RSER.2005.02.003

Basu, D. N., & Ganguly, A. (2016). Solar thermal-photovoltaic powered potato cold storage - Conceptual design and performance analyses. *Applied Energy*, *165*, 308–317. https://doi.org/10.1016/j.apenergy.2015.12.070

Boudéhenn, F., Demasles, H., Wyttenbach, J., Jobard, X., Chèze, D., & Papillon, P. (2012). Development of a 5 kW Cooling Capacity Ammonia-water Absorption Chiller for Solar Cooling Applications. *Energy Procedia*, *30*, 35–43. https://doi.org/10.1016/j.egypro.2012.11.006

Bux, S., & Ansari, E. A. (2017). Performance Analysis Vapour Absorption Refrigeration Chiller Run by Solar Thermal Energy. *International Journal of Advanced Engineering Research and Science*, *4*(10), 89–96. https://doi.org/10.22161/ijaers.4.10.15

Çengel, Y. A., & Boles, M. A. (2014). *Thermodynamics: An Engineering Approach* (8th ed.). McGraw-Hill Education.

Fadiel, A. F. A., & Esham, Y. A. M. (2023). *Absorption Refrigeration Cycle Technology*. https://doi.org/http://dx.doi.org/10.5772/intechopen.1001585

Gado, M. G., Megahed, T. F., Ookawara, S., Nada, S., & El-Sharkawy, I. I. (2021). Performance and economic analysis of solar-powered adsorption-based hybrid

cooling systems. *Energy Conversion and Management*, *238*. https://doi.org/10.1016/j.enconman.2021.114134

Gazda, W., & Kozioł, J. (2013). The estimation of energy efficiency for hybrid refrigeration system. *Applied Energy*, *101*, 49–57. https://doi.org/10.1016/j.apenergy.2012.05.006

Hackett, B., Chow, S., & Ganji, A. R. (2005). *Energy Efficiency Opportunities in Fresh Fruit and Vegetable Processing/Cold Storage Facilities*.

Han, W., Sun, L., Zheng, D., Jin, H., Ma, S., & Jing, X. (2013). New hybrid absorption-compression refrigeration system based on cascade use of mid-temperature waste heat. *Applied Energy*, *106*, 383–390. https://doi.org/10.1016/j.apenergy.2013.01.067

He, Y., & Chen, G. (2007). Experimental study on an absorption refrigeration system at low temperatures. *International Journal of Thermal Sciences*, *46*(3), 294–299. https://doi.org/10.1016/j.ijthermalsci.2006.06.002

Hera, D., & Vasilescu, C. (2011). *SOFTWARE APPLICATION FOR AN AMMONIA-WATER ABSORPTION HEAT PUMP USED FOR PERFORMANCE EVALUATION*.

Hera, D., Vasilescu, C., & Ferreira, C. I. (2010). Modular dynamic model for absorption systems simulation Model dinamic modular pentru simularea sistemelor cu absorbtie. In *Revista Română de Inginerie Civilă* (Vol. 1, Issue 2).

Herold, K. E., Radermacher, R., & Klein, S. A. (2016). *ABSORPTION CHILLERS AND HEAT PUMPS* (Second). https://boilersinfo.com

Jesús Cerezo Román, Rosenberg Javier Romero Domínguez, Antonio Rodríguez Martínez, & Pedro Soto Parra. (2019, February 22). *Thermal Analysis of an Absorption and Adsorption Cooling Chillers Using a Modulating Tempering Valve*.

Jog, K. V. (2004). Cold storage industry in India. *Proceedings of Refrigerated Warehouse \& Transport Association of Australia*, 1–21.

Kim, D. S., & Infante Ferreira, C. A. (2008). Solar refrigeration options – a state-of-the-art review. *International Journal of Refrigeration*, *31*(1), 3–15. https://doi.org/10.1016/J.IJREFRIG.2007.07.011

Liu, X., Ye, Z., Bai, L., & He, M. (2019). Performance comparison of two absorption-compression hybrid refrigeration systems using R1234yf/ionic liquid as working pair. *Energy Conversion and Management*, *181*, 319–330. https://doi.org/10.1016/j.enconman.2018.12.030

Selvaraj, D. A., & Victor, K. (2021). Design and Performance of Solar PV Integrated Domestic Vapor Absorption Refrigeration System. *International Journal of Photoenergy*, *2021*. https://doi.org/10.1155/2021/6655113

Sengupta, M., Xie, Y., Lopez, A., Habte, A., Maclaurin, G., & Shelby, J. (2018). The National Solar Radiation Data Base (NSRDB). In *Renewable and Sustainable Energy Reviews* (Vol. 89, pp. 51–60). Elsevier Ltd. https://doi.org/10.1016/j.rser.2018.03.003

Sharma, M. (2016). Analytical Study of Ammonia-Water (NH3-H2O) Vapor Absorption Refrigeration System Based On Solar Energy. In *Imperial Journal of Interdisciplinary Research*. http://www.onlinejournal.in

Srikhirin, P., Aphornratana, S., & Chungpaibulpatana, S. (2001). A review of absorption refrigeration technologies. In *Renewable and Sustainable Energy Reviews* (Vol. 5). www.elsevier.com/locate/rser

Wang, J., Wang, B., Wu, W., Li, X., & Shi, W. (2016). Performance analysis of an absorption-compression hybrid refrigeration system recovering condensation heat for generation. *Applied Thermal Engineering*, *108*, 54–65. https://doi.org/10.1016/j.applthermaleng.2016.07.100

Appendices

Appendix A

Figures of Study

Figure A.1

Configuration-I (Hybrid Adsorption-Vapor Compression Cooling System Integrated with Thermal Solar Energy System)

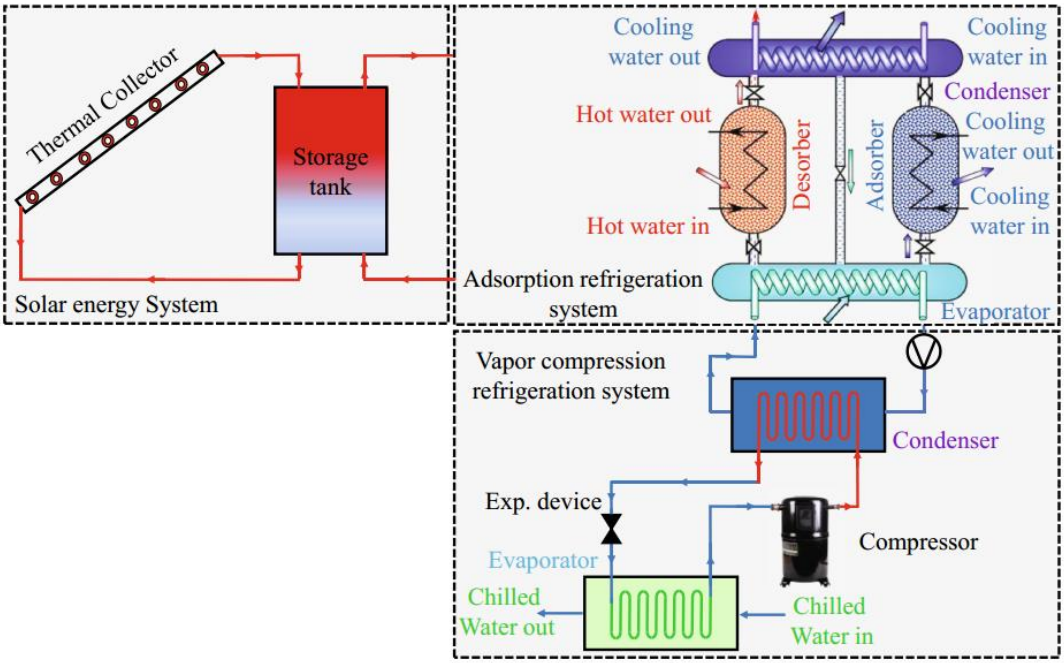

Figure A.2

Configuration-II (Hybrid Adsorption-Vapor Compression Cooling System Integrated with Thermal Solar Energy and Photovoltaic Solar Energy System)

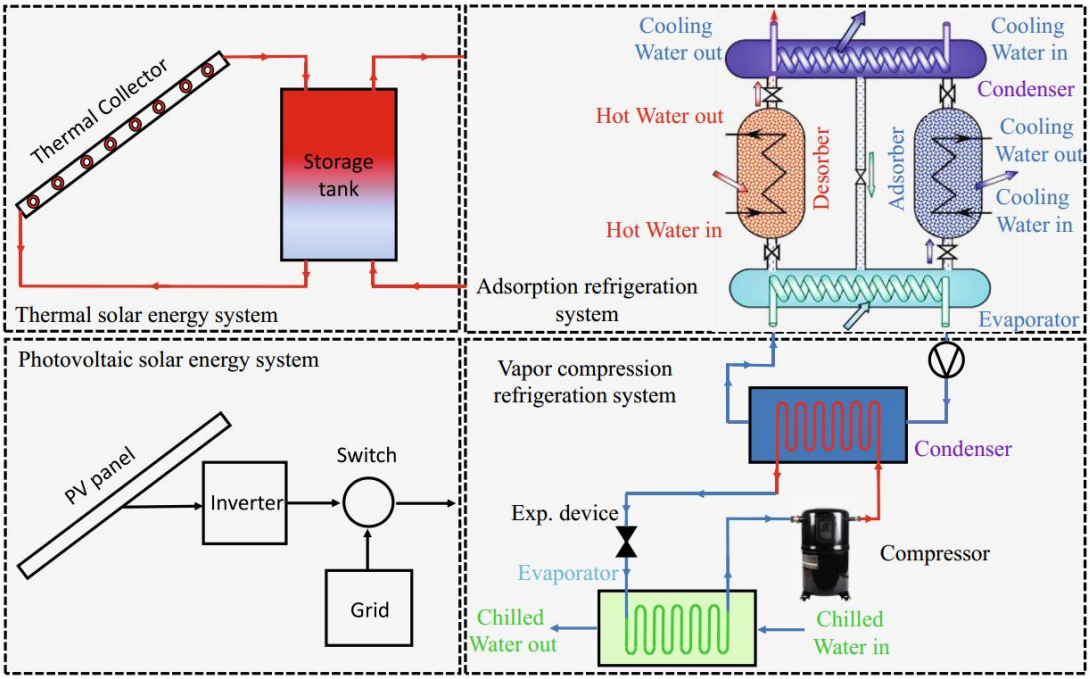

Figure A.3

Configuration-III (Solar-Assisted Hybrid Adsorption-Vapor Compression Cooling System Integrated with A Cold Storage Tank)

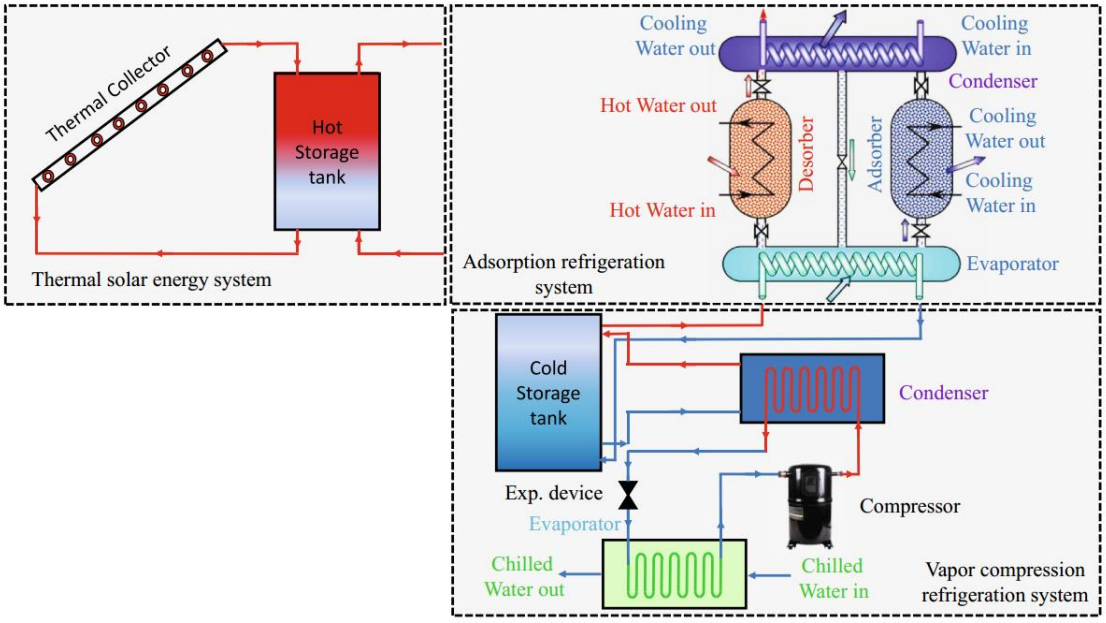

Figure A.4

Energy and mass flows at the compressor

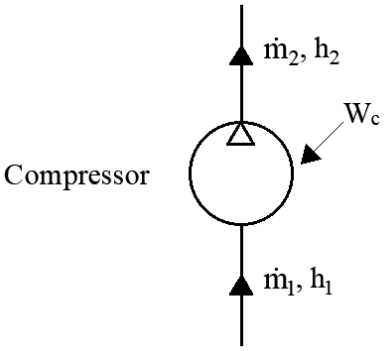

Figure A.5

Energy and mass flows at the condenser

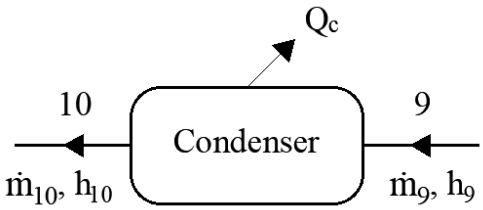

Figure A.6

Energy and mass flows at the expansion valve

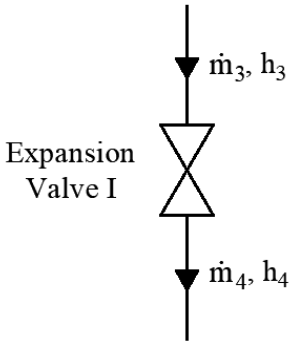

Figure A.7

Energy and mass flows at the evaporates

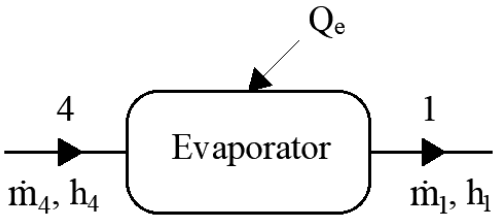

Figure A.8

Load calculations by Cool Pack software

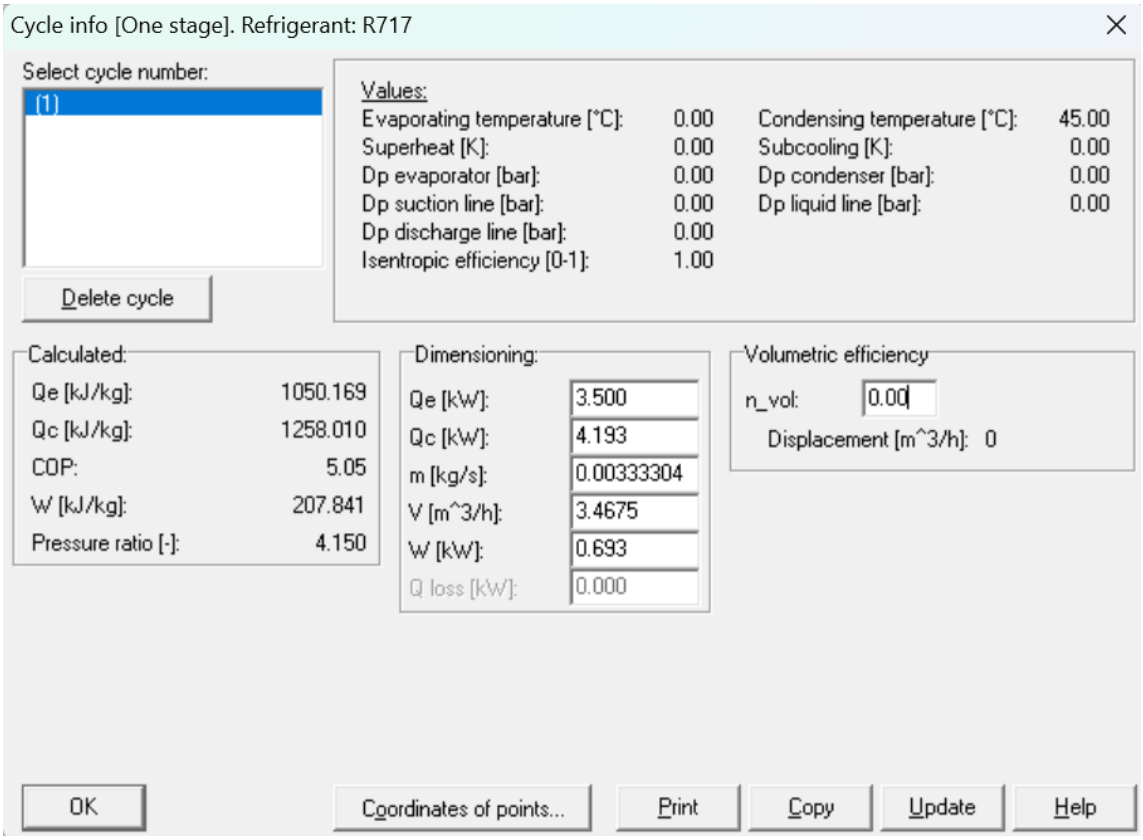

Figure A.9

Sate properties of the refrigeration cycle by EES

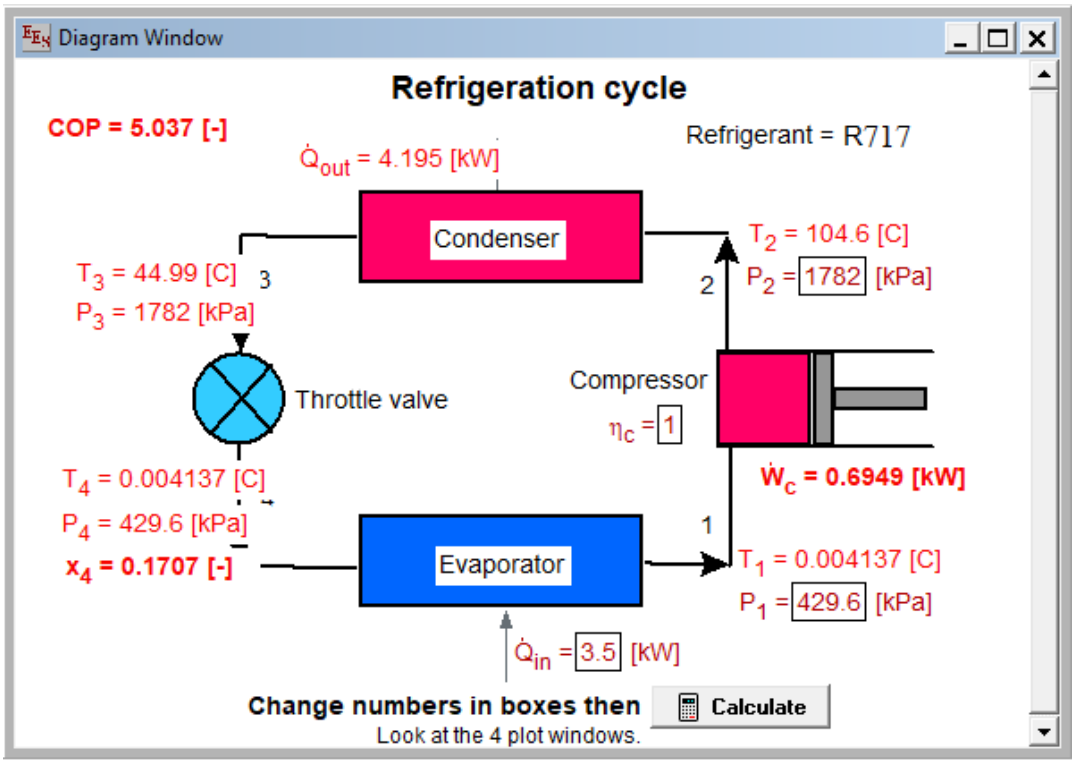

Figure A.10

Thermodynamic properties of each point by EES

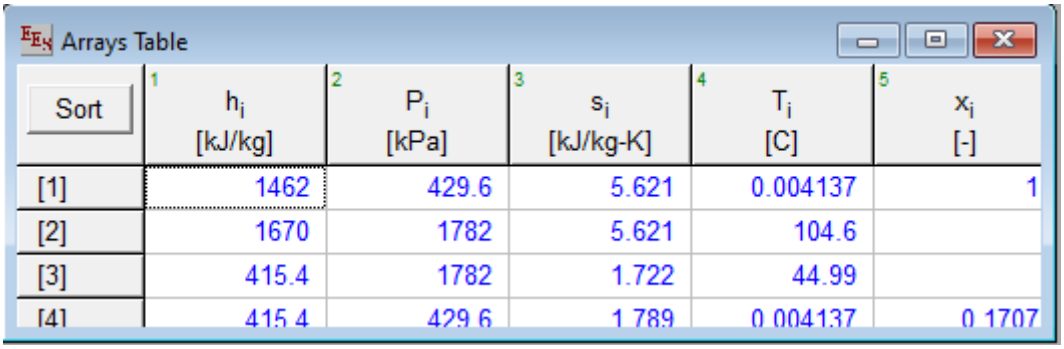
Arrays Table

Sort	1 h_i [kJ/kg]	2 P_i [kPa]	3 s_i [kJ/kg-K]	4 T_i [C]	5 x_i [-]
[1]	1462	429.6	5.621	0.004137	1
[2]	1670	1782	5.621	104.6	
[3]	415.4	1782	1.722	44.99	
[4]	415.4	429.6	1.789	0.004137	0.1707

Figure A.11

Energy and mass flows at the generator

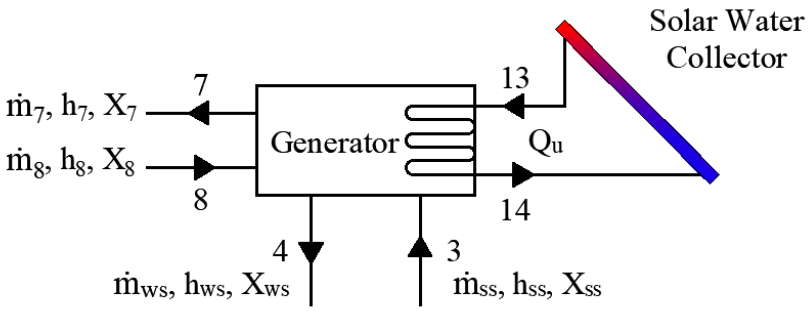

Figure A.12

Energy and mass flows at the rectifier

Figure A.13

Energy and mass flows at the absorber

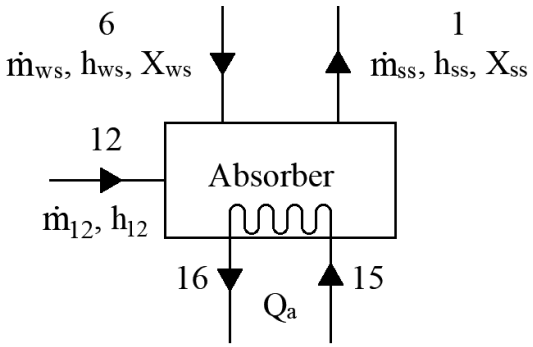

Figure A.14

Energy and mass flows at the heat exchanger

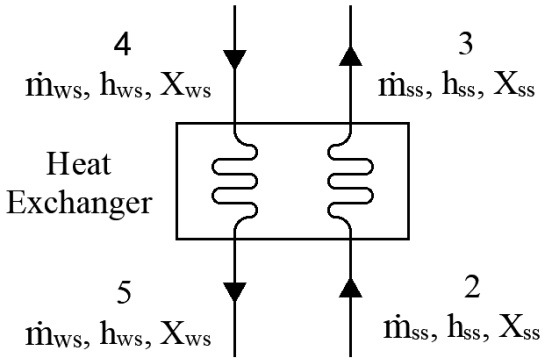

Figure A.15

Thermodynamic properties of ARS by EES software

Arrays Table

Sort	1 h_i [kJ/kg]	2 m_i [kg/s]	3 p_i [kPa]	4 Q_i	5 s_i [kJ/kg/K]	6 t_i [C]	7 v_i [m³/kg]	8 x_i [kg/kg]
[1]	-35.057	0.022	429.621	0.000	0.518	45.000	0.001	0.438304
[2]	-31.813	0.022	1781.945	-0.001	0.524	45.484	0.001	0.438304
[3]	257.183	0.022	1781.945	0.023	1.350	102.115	0.003	0.438304
[4]	332.876	0.019	1781.945	0.000	1.518	121.075	0.001	0.338304
[5]	-7.571	0.019	1781.945	-0.001	0.562	45.484	0.001	0.338304
[6]	-7.571	0.019	429.621	-0.001	0.567	45.745	0.001	0.338304
[7]	1490.421	0.004	1781.945	1.000	4.684	99.627	0.093	0.969428
[8]	215.764	0.000	1781.945	0.000	1.240	99.649	0.001	0.438304
[9]	1292.919	0.003	1781.945	1.000	4.117	44.950	0.073	1.000000
[10]	216.038	0.003	1781.945	0.000	0.735	45.000	0.002	1.000000
[11]	216.038	0.003	1781.945	0.000	0.735	44.950	0.002	1.000000
[12]	216.038	0.003	429.621	0.170	0.799	0.013	0.051	1.000000
[13]	1268.295	0.003	429.621	1.000	4.633	0.000	0.289	1.000000
[14]	1268.295	0.003	429.621	1.000	4.633	0.015	0.289	1.000000

Figure A.16

ETC technical data sheet

Collector type	HP10-1000	HP20-2000	HP30-3000
Performance Power Plus *1	1000 Wpeak	2000 Wpeak	3000 Wpeak
Aperture area Power Plus	1,487 m^2	2,974 m^2	4,461 m^2
η_0 Power Plus *1	0,68	0,68	0,68
Performance Power *2	717 Wpeak	1434 Wpeak	2151 Wpeak
Aperture area Power	1,017 m^2	2,034 m^2	3,051 m^2
η_0 Power *2	0,70	0,70	0,70
Number of vacuum tubes	10 Stk.	20 Stk.	30 Stk.
Length Ⓐ	2210 mm	2210 mm	2210 mm
Width Ⓑ	750 mm	1500 mm	2250 mm
Height Ⓒ	88 mm	88 mm	88 mm
Gross area	1,66 m^2	3,32 m^2	4,97 m^2
Weight	25,24 kg	50,48 kg	75,72 kg
Vacuum in the tube (100% insolated)	10^{-5} mbar	10^{-5} mbar	10^{-5} mbar
Fluid volume	0,47 l	0,94 l	1,41 l
Collector flow rate	0,68-0,83 l/min.	1,37-1,66 l/min.	2,05-2,48 l/min.
Pressure loss with flow rate	2 mbar	6 mbar	22 mbar
Max. operating pressure	10 bar	10 bar	10 bar
Max. collector stagnation temperature	158° C	158° C	158° C
Collector connection	18 mm Ø	18 mm Ø	18 mm Ø
Collector installation (tube)	min. 20° max. 90°	min. 20° max. 90°	min. 20° max. 90°
Heat carrier fluid	S-SOL-VT^{50}	S-SOL-VT^{50}	S-SOL-VT^{50}

*1 Peak performance as per Keymark, with a solar irradiation of 985 W/m^2 and a radiation angle of 15° in relation to the aperture area absorber fin of vacuum tubes are coated on both sides.

*2 Peak performance as per "Keymark", with a solar irradiation of 985 W/m^2 and a radiation angle of 15° in relation to the aperture area absorber fin of vacuum tubes is coated on one side.

Figure A.17

ACHRS working hours annually

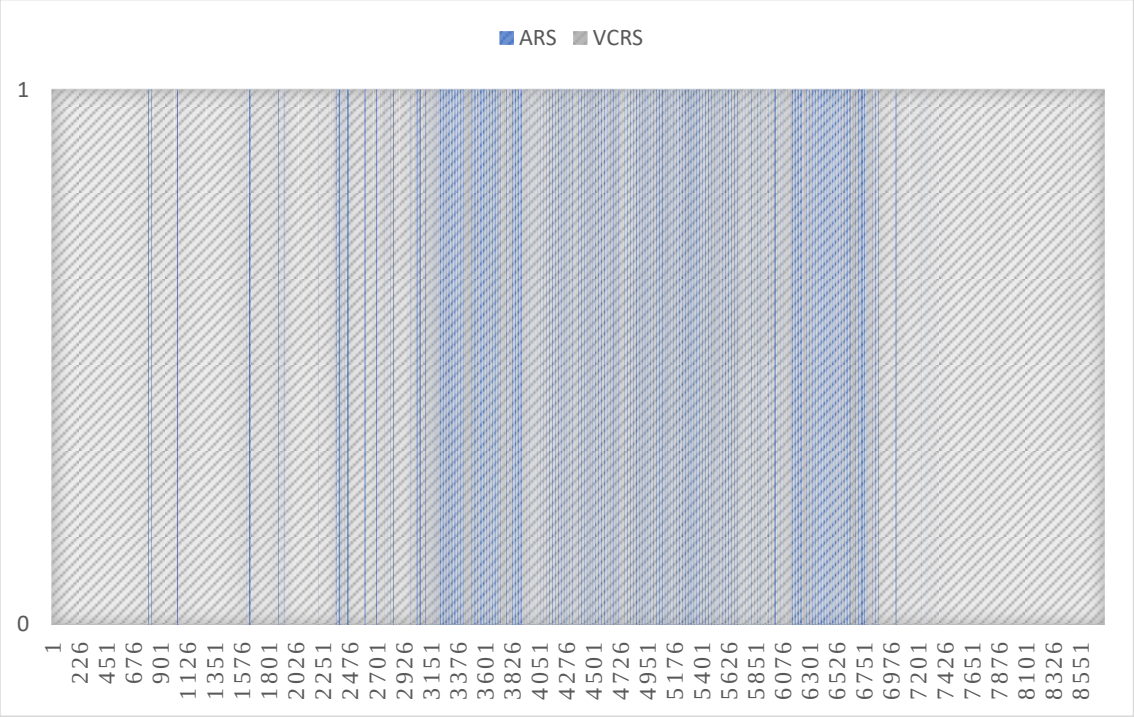

Appendix B

P-h Diagram for R717 Refrigerant

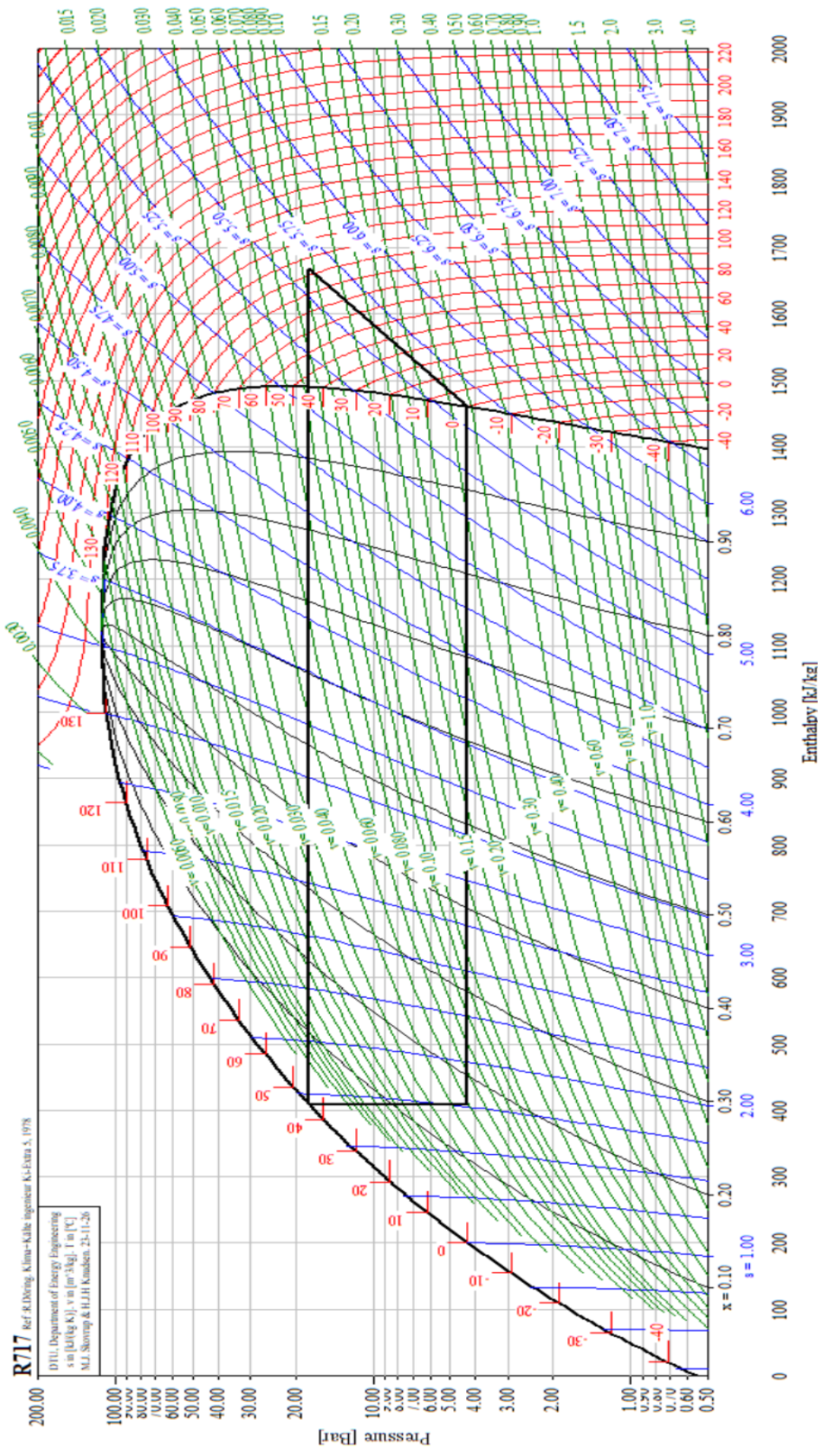

Appendix C

EES Window for Absorption Refrigeration System Equations

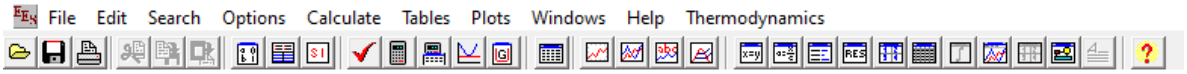


```
PROCEDURE TPQ(TC,P,Q:x,h,v,s)
"given T (temperature), P (pressure) and Q (quality) in SI units,
 this procedures returns x, h, v and s in SI units"
TK=TC+273.15
Pbar=P*.01
CALL NH3H2O(128,TK,Pbar,Q:TK,Pbar,x,h,s,u,v,Q)
END
PROCEDURE TPX(TC,P,x:Q,h,v,s)
"given T (temperature), P (pressure) and x (ammonia wt fraction) in SI
units, this procedure returns Q, h, v and s in SI units"
TK=TC+273.15
Pbar=P*.01
CALL NH3H2O(123,TK,Pbar,x:TK,Pbar,x,h,s,u,v,Q)
END
PROCEDURE PXQ(P,x,Q:TC,h,v,s)
"given P (pressure in bar), x (ammonia wt fraction) and Q, this procedure
 returns T, h, v and s in SI units"
Pbar=P*.01
CALL NH3H2O(238,Pbar,x,Q:TK,Pbar,x,h,s,u,v,Q)
TC=TK-273.15
END
PROCEDURE PHX(P,h,x:TC,Q,v,s)
"given P (pressure in bar), enthalpy (J/g), and x (ammonia wt
fraction), this procedure returns T, Q, v and s in SI units"
Pbar=P*.01
CALL NH3H2O(234,Pbar,x,h:TK,Pbar,x,h,s,u,v,Q)
TC=TK-273.15
END
PROCEDURE TXQ(TC,x,Q:P,h,v,s)
"given T (temperature in C), Q (quality) and x (ammonia wt fraction) in SI
units, this procedure returns P, h, v  and s in SI units"
TK=TC+273.15
CALL NH3H2O(138,TK,x,Q:TK,Pbar,x,h,s,u,v,Q)
P=Pbar*100
END
PROCEDURE PXS(P,x,s:TC,h,v,Q)
"given P (pressure in bar), x (ammonia wt fraction) and entropy s, this procedure
 returns T, h, v and Q in SI units"
Pbar=P*.01
CALL NH3H2O(235,Pbar,x,s:TK,Pbar,x,h,s,u,v,Q)
TC=TK-273.15
END

"This procedure calculates the amount of heat that is exchanged
in the solution heat exchanger"
PROCEDURE SHX(eshx,mls,mrs,ha,hb,hc,hd:hcc,hdd,qshx)
qls=mls*(hd-ha) "amount of heat on 'left side', rich solution"
qrs=mrs*(hb-hc)  "amount of heat on 'right side', poor solution"
qmin=MIN(qls,qrs)
qshx=eshx*qmin  "eshx is the sol. hx. effectiveness"
 hcc=hb-eshx*qmin/mrs  "calculation of outlet enthalpies"
 hdd=ha+eshx*qmin/mls
END
```

```
"INPUT PARAMETERS"
"efficiencies"
etap=0.50 "isentropic efficency of pump"
eshx=1 "solution heat exchanger efectiveness"
esc=0.0 "effectiveness of condensate precooler, if esc=0, no
subcooler is used"
f=(x[9]-x[4])/(x[3]-x[4]) "solution circulation ratio"
"temperatures"
t[13]=0  " for state point, see diagram window"
t[10]=45
t[1]=45
tglide=T[13]-T[12]
"mass fractions"
x[9]=1
x[1]-x[4]=Dx
Dx=0.1
"mass flow "
m[9]=0.00333
"Quality"
Q[13]=1
Q[10]=0.00
Q[7]=1
Q[9]=1
Q[1]=0
Q[4]=0

"governing equations"
"ABSORBER"
m[14]+m[6]=m[1]
m[14]*x[14]+m[6]*x[6]=m[1]*x[1]
m[14]*h[14]+m[6]*h[6]=m[1]*h[1]+Qabs
"DESORBER"
balm=m[8]+m[3]-(m[7]+m[4])
bala=m[8]*x[8]+m[3]*x[3]-(m[7]*x[7]+m[4]*x[4])
m[3]*h[3]+m[8]*h[8]+Qgen=m[7]*h[7]+m[4]*h[4]
CALL pxq(P[3],x[3],0:T3f,h3f,v3f,s3f)
T[7]=T3f
"RECTIFIER"
m[7]=m[9]+m[8]
m[7]*x[7]=m[9]*x[9]+m[8]*x[8]
m[7]*h[7]=m[9]*h[9]+m[8]*h[8]+Qrect
h[8]=h3f
x[8]=x[3]
"PUMP"
swp=v[1]*(p[2]-p[1])/etap
h[2]=h[1]+swp
Wp=m[1]*(h[2]-h[1])
"EXPANSION VALVE"
h[5]=h[6]
"SHX"
CALL tpx(T[2],P[5],x[5]:Q5e,h5e,v5e,s5e)
CALL tpx(T[4],P[3],x[3]:Q3e,h3e,v3e,s3e)
CALL shx(eshx,m[2],m[4],h[2],h[4],h5e,h3e:h[5],h[3],Qshx)
"CONDENSER"
Qcond=m[9]*(h[9]-h[10])
"EVAPORATOR"
Qevap=m[13]*(h[13]-h[12])
```

```
"EXPANSION VALVE"
h[11]=h[12]
"C-E HX"
CALL tpx(t[10],P[14],x[14]:Q14e,h14e,v14e,s14e)
CALL tpx(t[13],P[11],x[11]:Q11e,h11e,v11e,s11e)
CALL shx(esc,m[13],m[10],h[13],h[10],h11e,h14e:h[11],h[14],QCE)
"OVERALL"
COP=Qevap/(Wp+Qgen)
checkQ=Qgen+Qevap+Wp-(Qrect+Qcond+Qabs)
pratio=phigh/plow
"SET PRESSURES"
p[1]=plow
p[2]=phigh
P[3]=phigh
p[4]=phigh
P[5]=phigh
P[6]=plow
p[7]=phigh
p[8]=phigh
p[9]=phigh
p[10]=phigh
p[11]=phigh
p[12]=plow
P[13]=plow
P[14]=plow
"TRIVIAL MASS BALANCES"
m[1]=m[2]
m[2]=m[3]
m[4]=m[5]
m[5]=m[6]
m[9]=m[10]
m[10]=m[11]
m[11]=m[12]
m[12]=m[13]
m[13]=m[14]
"TRIVIAL NH3 BALANCES"
x[1]=x[2]
x[2]=x[3]
x[4]=x[5]
x[5]=x[6]
x[9]=x[10]
x[10]=x[11]
x[11]=x[12]
x[12]=x[13]
x[13]=x[14]
"STATE POINTS"
CALL txq(t[1],x[1],Q[1]:p[1],h[1],v[1],s[1])
CALL phx(p[2],h[2],x[2]:T[2],Q[2],v[2],s[2])
CALL phx(P[3],h[3],x[3]:T[3],Q[3],v[3],s[3])
CALL pxq(p[4],x[4],Q[4]:T[4],h[4],v[4],s[4])
CALL phx(P[5],h[5],x[5]:T[5],Q[5],v[5],s[5])
CALL phx(P[6],h[6],x[6]:T[6],Q[6],v[6],s[6])
CALL tpq(T[7],p[7],Q[7]:x[7],h[7],v[7],s[7])
CALL phx(p[8],h[8],x[8]:T[8],Q[8],v[8],s[8])
CALL pxq(p[9],x[9],Q[9]:T[9],h[9],v[9],s[9])
CALL txq(t[10],x[10],Q[10]:p[10],h[10],v[10],s[10])
CALL phx(p[11],h[11],x[11]:T[11],Q[11],v[11],s[11])
CALL phx(p[12],h[12],x[12]:t[12],q[12],v[12],s[12])
CALL txq(t[13],x[13],q[13]:p[13],h[13],v[13],s[13])
CALL phx(P[14],h[14],x[14]:T[14],Q[14],v[14],s[14])
```

جامعة النجاح الوطنية

كلية الدراسات العليا

تقييم إستهلاك الطاقة لنظام التبريد الهجين بالإمتصاص وإنضغاط البخار لغرف التبريد

إعداد

إبراهيم عبد الرحيم محمد عمايرة

إشراف

د. عبد الرحيم أبو الصفا

قدمت هذه الرسالة استكمالاً لمتطلبات الحصول على درجة الماجستير في هندسة الطاقة النظيفة وترشيد الاستهلاك، من كلية الدراسات العليا، في جامعة النجاح الوطنية، نابلس – فلسطين.

2024

تقييم إستهلاك الطاقة لنظام التبريد الهجين بالإمتصاص وإنضغاط البخار لغرف التبريد

إعداد

إبراهيم عبد الرحيم محمد عمايرة

إشراف

د. عبد الرحيم أبو الصفا

الملخص

إن العديد من المتغيرات المترابطة التي تؤثر على البيئة والاقتصاد ورفاهية العالم ككل تحتاج إلى استخدام الطاقة المتجددة. وبناء على ذلك، تمت دراسة نظام التبريد الهجين ذو الضغط الامتصاصي (ACHRS) في هذا البحث. ونظراً لإرتفاع تكلفة الطاقة الكهربائية والمناخ الملائم لتجميع الطاقة الشمسية، فقد بدا من العملي والمجدي اقتصادياً إيجاد طريقة مختلفة لتشغيل غرف التبريد مع الحفاظ على آداء النظام. يقوم ACHRS بدمج نظام التبريد بإنضغاط البخار (VCRS)، ونظام التبريد بالامتصاص (ARS)، بالإعتماد على درجة حرارة الماء الناتجة عن التسخين باستخدام السخانات الشمسية ذات الأنابيب المفرغة، عندما تكون درجة حرارة الماء 90 درجة مئوية وأكثر، فسيعمل النظام عن طريق ARS، وإلا عن طريق VCRS. أظهرت نتائج الدراسة أن ساعات العمل السنوية للنظام الهجين ستكون 2078 بنظام ARS و6682 بنظام VCRS. فترة الإسترداد للنظام الهجين هي 5.6 سنوات. يعتبر صافي التدفق النقدي (NCF)، ومعدل العائد الداخلي (IRR) من الطرق الأخرى لتقييم الجدوى الاقتصادية التي تمت دراستها، ومن خلالها تم إثبات الجدوى الاقتصادية للنظام.

الكلمات المفتاحية: التبريد بالامتصاص؛ الجدوى الاقتصادية؛ الأنابيب المفرغة؛ التبريد الهجين؛ طاقة شمسية.